Cell Reports
Medicine

Article

Bioengineering of a human iPSC-derived vascularized endocrine pancreas for type 1 diabetes

Graphical abstract

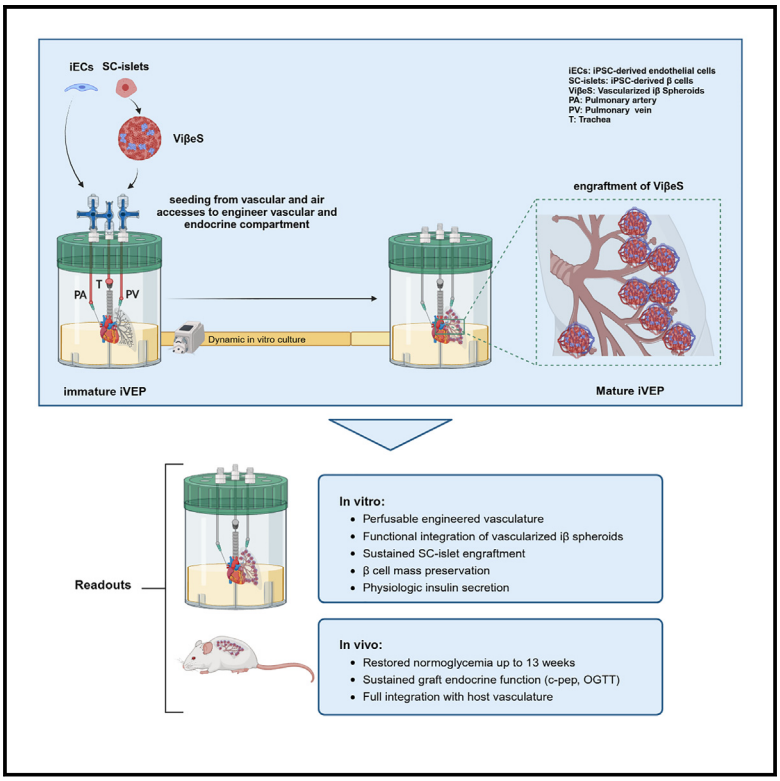

Highlights

- Assembly of functional vascularized iβ spheroids (ViβeSs) from differentiated human iPSC
- iVEP stems from decellularized lung ECM, iPSC-derived ViβeSs, and endothelial cells
- *In vitro*, iVEP improves endocrine and vascular survival and function
- *In vivo*, iVEP enhances fast engraftment restoring normoglycemia in diabetic mice

Authors

Francesco Campo, Alessia Neroni, Cataldo Pignatelli, ..., Vito Lampasona, Lorenzo Piemonti, Antonio Citro

Correspondence

citro.antonio@hsr.it

In brief

This study addresses the limitations of intrahepatic islet transplantation in type 1 diabetes by repurposing decellularized lungs into a human iPSC-based vascularized endocrine pancreas (iVEP). Campo et al. generate a functional organ that improves β cell function and survival *in vitro* and fast engraftment *in vivo*, advancing diabetes cell therapies.

Campo et al., 2025, Cell Reports Medicine *6*, 101938
February 18, 2025
https://doi.org/10.1016/j.xcrm.2025.101938

CellPress

Cell Reports Medicine

CellPress
OPEN ACCESS

Article

Bioengineering of a human iPSC-derived vascularized endocrine pancreas for type 1 diabetes

Francesco Campo,[1,4] Alessia Neroni,[1,4] Cataldo Pignatelli,[1] Silvia Pellegrini,[1] Ilaria Marzinotto,[1] Libera Valla,[1,2,3] Fabio Manenti,[1] Martina Policardi,[1] Vito Lampasona,[1] Lorenzo Piemonti,[1,4] and Antonio Citro[1,5,6,*]

[1]San Raffaele Diabetes Research Institute, IRCCS San Raffaele Scientific Institute, Milan, Italy
[2]Chair for Molecular Animal Breeding and Biotechnology, Gene Center and Department of Veterinary Sciences, LMU Munich, 81377 Munich, Germany
[3]Center for Innovative Medical Models (CiMM), LMU Munich, 85764 Oberschleißheim, Germany
[4]Università Vita-Salute San Raffaele, Milan, Italy
[5]X (formerly Twitter): @Citro_Lab
[6]Lead contact
*Correspondence: citro.antonio@hsr.it
https://doi.org/10.1016/j.xcrm.2025.101938

SUMMARY

Intrahepatic islet transplantation in patients with type 1 diabetes is limited by donor availability and lack of engraftment. Alternative β cell sources and transplantation sites are needed. We demonstrate the feasibility to repurpose a decellularized lung as an endocrine pancreas for β cell replacement. We bioengineer an induced pluripotent stem cell (iPSC)-based version, fabricating a human iPSC-based vascularized endocrine pancreas (iVEP) using iPSC-derived β cells (iPSC-derived islets [SC-islets]) and endothelial cells (iECs). SC-islets and iECs are aggregated into vascularized iβ spheroids (ViβeSs), and over 7 days of culture, spheroids integrate into the bioengineered vasculature, generating a functional, perfusable human endocrine organ. *In vitro*, the vascularized extracellular matrix (ECM) sustained SC-islet engraftment and survival with a significantly preserved β cell mass and a physiologic insulin release. *In vivo*, iVEP restores normoglycemia in diabetic NSG mice. We report a human iVEP providing a controlled *in vitro* insulin-secreting phenotype and *in vivo* function.

INTRODUCTION

Type 1 diabetes (T1D) is a global disease burden, affecting more than 8.4 million patients worldwide.[1] Although the primary treatment for patients with T1D is the combination of glucose monitoring coupled with daily exogenous insulin injection, they still suffer due to the challenge associated with daily compliance and T1D secondary effects.[2] Daily insulin injection imperfectly simulates the dynamic glucose/insulin homeostasis control mediated by the pancreatic islets in response to changes in blood glucose concentration.[3] An available option is the β cell replacement therapy. As of now, donor organ shortage and the immune reaction against the graft limit its application.[4] Recently, new protocols for *in vitro* differentiation of human pluripotent stem cells (hPSCs) into functional pancreatic β and endothelial cells were reported,[5–9] opening the field to a new chapter with an unlimited supply of human insulin-producing vascularized tissues. Additionally, growing evidence reported that the microenvironment plays a crucial role in cell behavior, differentiation, and function.[10] Extracellular matrix (ECM) components can induce and promote intracellular biochemical signaling.[11,12] Thus, ECM geometry and stiffness resulted as key players in modulating stem cell differentiation, suggesting that the use of decellularized native organ ECM could positively impact the maturation of hPSC into β cells.[13] Of note, recent clinical trials in the field of stem cell as β cell replacement strategy (NCT05791201, NCT03163511), although in the presence of synthetic and not ECM-based device, showed an intriguing future for this application with room for improvement in scaffold design.[14,15] Major efforts were made to optimize organ decellularization protocols aimed to generate inert biological scaffolds with preserved native organ ECM composition, three-dimensional (3D) architecture, and perfusable vascular bed.[16–21] We previously reported the possibility to merge organ decellularization technology with the β cell replacement purpose with the final aim of engineering a functional xenogeneic vascularized endocrine pancreas (VEP) using immature neonatal porcine islets as a source of insulin-producing cells and healthy-subject-derived blood outgrowth endothelial cells.[22] This platform was able not only to foster neonatal pig islet (NPI) maturation *in vitro* but also to perform upon transplantation *in vivo*, in immunocompromised NSG mouse models, for over 18 weeks compared to available preclinical models. Herein, we demonstrated the plasticity of our technology by bioengineering a human induced pluripotent stem cell (iPSC)-based VEP (iVEP). We found that our platform offers valuable support to integrate terminal

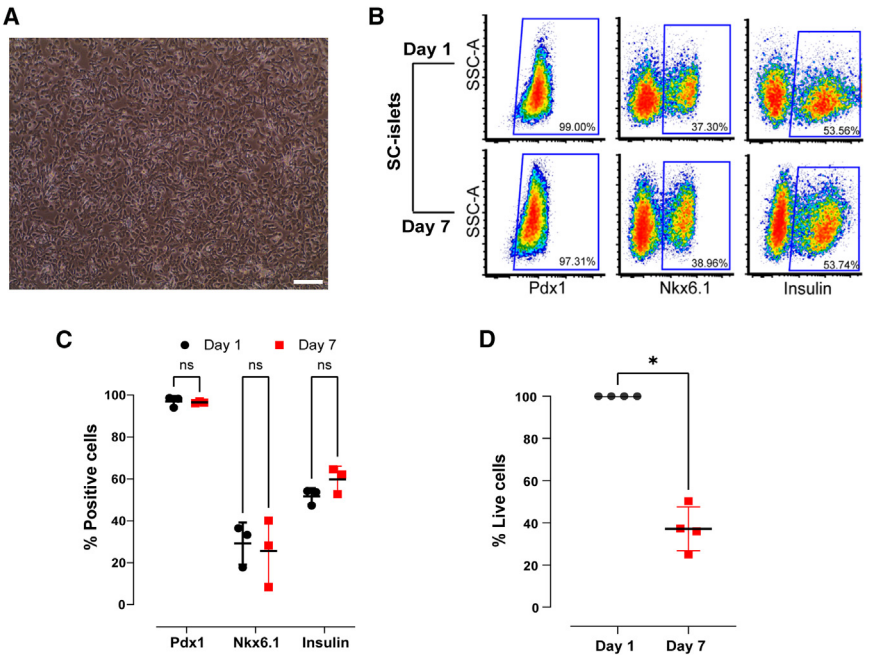

Figure 1. SC-islet characterization for iVEP assembly

(A) Representative bright-field image of SC-islets in standard culture condition.

(B) Representative SC-islet flow cytometry characterization for Pdx1, Nkx6.1, and insulin at day 1 and day 7 post culture.

(C) Flow cytometry quantification of Pdx1, Nkx6.1, and insulin expression in SC-islets at day 1 and day 7 after standard culture (values are presented as mean ± SD, Pdx1: day 1 96.95% ± 2.57% vs. day 7 96.48% ± 0.44%, Nkx6.1: day 1 29.17% ± 10.04% vs. day 7 25.62% ± 16.056%, and insulin: day 1 51.74% ± 3.86% vs. day 7 59.85% ± 6.27%; $n = 3$ biological replicates; two-way ANOVA).

(D) Quantification of SC-islet live cells after 7 days of culture (*100% at day 1 vs. 37.16% ± 10.38% at day 7; values are presented as mean ± SD, $n = 4$ biological replicates, Mann-Whitney U test $p = 0.0286$).

differentiated human iPSC-derived islets (SC-islets) and iPSC-derived endothelial cells (iECs). To foster organ vascular and endocrine compartment integration, SC-islets and iECs were aggregated into functional vascularized endocrine spheroids and then seeded in a pre-vascularized lung scaffold cultured over 7 days. The dedicated organ maturation culture protocol allowed the preservation of the differentiated phenotype and the improvement in vascular and endocrine function. Moreover, we found that the *in vitro* engraftment of insulin-producing cells in a pre-vascularized decellularized ECM environment shows an immediate and sustained *in vivo* function compared to the deviceless (DL) site, a pre-vascularized implantation model.

RESULTS

iPSC-derived β cell and iEC validation in iVEP culture condition

To develop a functional pre-vascularized endocrine organ, we matured scaffolds by seeding iECs and SC-islets under dynamic perfusion culture over 7 days. SC-islets were purchased from Takara Bio (https://www.takarabio.com) while iECs from Fujifilm Cellular Dynamics (https://www.fujifilmcdi.com), so two different donor cells were used to engineer our platform. As a preliminary step, we firstly evaluated the persistency of the iEC phenotype and SC-islet identity after 7 days of standard culture conditions, and we did not observe significant differences. SC-islets preserved the expression of markers of differentiated β cells in flow cytometry (Pdx1: day 1 96.95% ± 2.57% and day 7 96.48% ± 0.44%; Nkx6.1: day 1 29.17% ± 10.04% and day 7 25.62% ± 16.056%; insulin: day 1 51.74% ± 3.86% and day 7 59.85% ± 6.27%) (Figures 1A–C and S1) ($n = 3$ biological replicates). Moreover, SC-islets showed a consistent and significant reduction in cell number during 7 days of standard culture (percentage of live cells from 100% at day 1 to 37.16% ± 10.38% at day 7; $p = 0.0286$) (Figure 1D). iECs retained their expression of endothelial markers as shown by flow cytometry ($CD31^+/CD105^+/CD73^+/CD90^-$) (see Figures 2A, 2B, and S2), a finding further supported by immunofluorescence staining ($CD31^+/CD144^+$) for endothelial phenotype confirmation (Figure 2D). Additionally, we evaluated the performance of iECs under iVEP culture conditions against standard culture media, specifically angiogenic medium (AM), modified stabilization medium (MSM), and VascuLife medium,[20,22,23] focusing on the preservation of their phenotype (Figures 2C and S2), proliferation rate (Figure 2E), and function capabilities (Figures 2F and 2G). iECs cultured in iVEP-specific media, including both AM and MSM, successfully retained their endothelial characteristics (Figure 2C). Using the Incucyte live-cell analysis system for the proliferation assays, we noted comparable proliferation rates of iECs in AM and MSM when contrasted with the VascuLife medium. The proliferation index, measured at each time point from the initial confluence at T0, revealed no significant variances (Figures 2E and S3), confirming an efficient iEC proliferation in iVEP media ($n = 2$ biological replicates). Furthermore, the functionality of iECs was tested through a tube formation assay across the different media ($n = 3$ biological replicates). No statistical significance was found in the performance of iEC tube formation (measured as the mean mesh size) when cultured in AM, MSM, or a combination of both, as compared to the VascuLife medium (Figure 2G).

iVEP assembly: iPSC vascular and endocrine compartment generation

Following the verification of SC-islet and iEC stability, we generated vascularized iβ spheroids (ViβeSs) by co-seeding SC-islets and iECs in a sphericalplate 5D, with a ratio of 90% SC-islets to 10% iECs (Figure 3A). ViβeSs were cultured for 7 days to allow their acclimatization and aggregation before being employed in iVEP bioengineering processes. Upon collection, ViβeSs exhibited uniformity in size, with an average diameter of 93.57 ± 24.7 μm across

CellPress
OPEN ACCESS

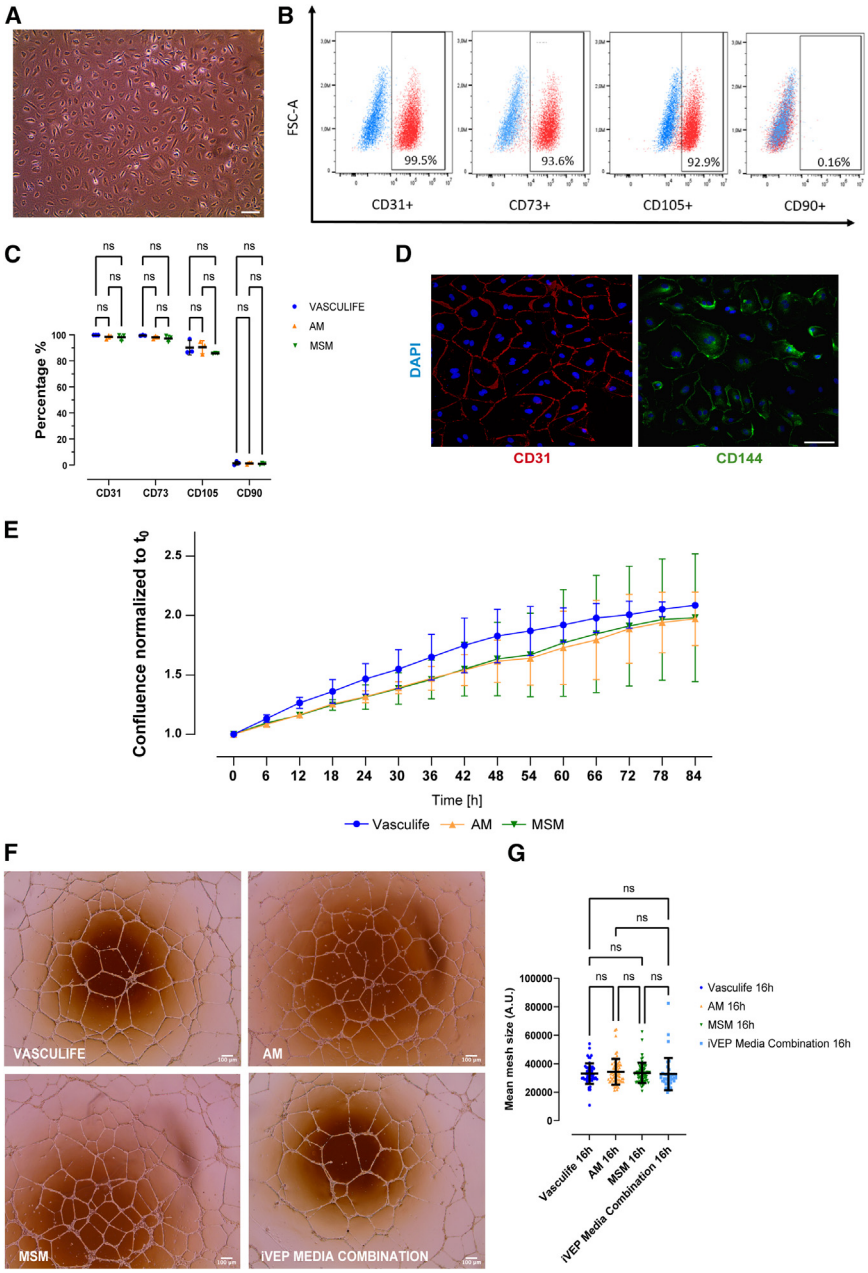

Figure 2. iEC characterization for iVEP assembly

(A) Representative bright-field image of iECs in standard culture condition.

(B) Representative iEC flow cytometry characterization for CD90, CD31, CD105, and CD73 post culture used for iVEP engineering.

(C) Flow cytometry quantification of CD90, CD31, CD105, and CD73 expression in iECs at different passages after standard culture in different culture media used for iVEP engineering (n = 3 biological replicates). Values are presented as mean ± SD.

(D) Immunofluorescence staining of iEC endothelial phenotyping CD31 (red), VE-cadherin (CD144, green), and DAPI (blue).

(E) Proliferation assay by Incucyte. Proliferation index of iECs in iVEP culture media (AM and MSM) vs. VascuLife medium as control, with respect to time 0 confluence. Values are presented as mean ± SD (n = 3 biological replicates).

(F) Representative images of iEC morphology in tube formation assays using iVEP media combination, modified stabilization medium (MSM), angiogenic medium (AM), and VascuLife medium. Magnification 4×.

(G) Tube formation assay quantification and analysis of the formed vascular mesh in VascuLife, AM, MSM, and iVEP media combination. Scale bars in μm (n = 3 independent experiments, biological replicates. For each condition (VascuLife, AM, MSM, and iVEP media combination), 56, 68, 69, and 39 images were acquired, respectively. Values are presented as mean ± SD.

8 independently analyzed batches (Figures 3A and 3B). iECs were tracked over acclimatization and aggregation phase using a fluorescent dye (fluo-dye) for Incucyte Live-cell analysis system (Figure 3C). During the ViβeS aggregation phase, we observed, according to the spheroid assembly process, an expected non-significant reduction in fluorescence intensity. After the aggregation window, we noticed strong stability of the iEC fluorescence signal, till the end of the assembly process, suggesting the unaltered endothelial cell mass within the formed ViβeSs (Figure 3C). Additionally, as shown by ViβeS aggregation time lapse, the spheroid assembly was confirmed starting from 48 h from the seeding (Video S1). Upon harvesting, the presence of both SC-islets, marked by Pdx1, Nkx6.1, chromogranin A (CHGA+), C-peptide (C-pep), and insulin (INS+), and iECs, identified by CD31^{+}, was confirmed (Figure 3D). To bioengineer iVEP, firstly, we repopulated acellular lung matrixes by seeding iEC from both the pulmonary artery (PA) and pulmonary vein, followed by culturing the re-endothelialized scaffolds in AM (Figure 4 A). On the subsequent day, we delivered, as already validated in our previous protocol,[22,23] a combination of ViβeSs and iECs into the lung via the trachea. During these procedures, we did not observe any cell spillage from the lung lobe architecture, confirming the decellularized rat lung left lobe ability to retain the seeded cells. We then cultured the assembled constructs for an additional 4 days in AM, followed by 2 days in MSM (Figure 4A). At the conclusion of the maturation process, we observed the formation of spatially organized, distinct tissue compartments. Thus, an endothelial cell network, marked by positivity for human von Willebrand Factor (vWF+), was established across the bioengineered organ, with ViβeSs integrated within the vascular framework (Figures 4B and S4). To investigate whether the developed vasculature architecture (Video S2) would allow direct perfusion of the iVEP structure, we tested vascular function by two different assays: FITC dextran assay and fluorangiography assay. For dextran assay, a matured scaffold seeded

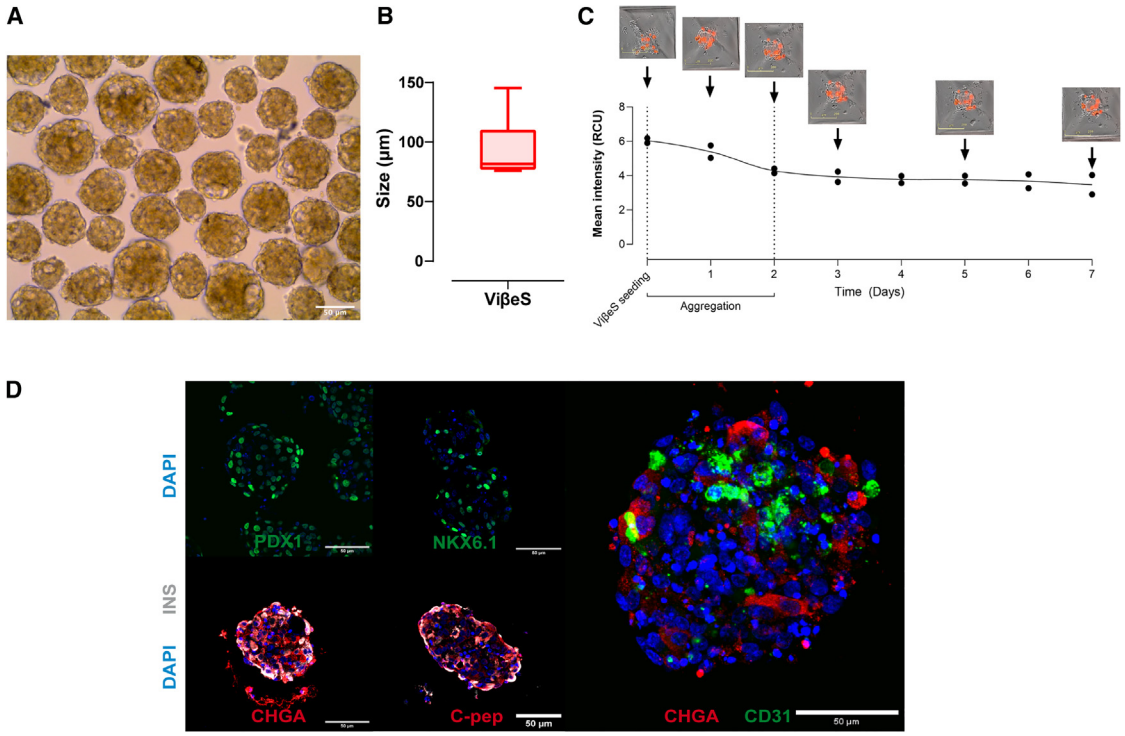

Figure 3. ViβeS characterization

(A) Representative image of ViβeSs at day 7 upon harvesting.

(B) ViβeS size quantification (n = 8 biological independent ViβeS replicates; for each replicate, the size of 42, 82, 29, 38, 33, 49, 62, and 57 spheroids were measured, respectively).

(C) ViβeS assembly longitudinal observation. iECs stained in red and observed during culture through fluorescence quantification by mean intensity. n = 2 biological replicates.

(D) Immunofluorescence staining of ViβeSs before seeding in iVEP: iECs positive for human CD31 in green, SC-islets positive for human Pdx1, human Nkx6.1 in green, human CHGA, human C-pep in red, and human insulin (INS) in gray.

with iECs exclusively, was perfused at 1 mL/min with an FITC-dextran solution (5 mg/mL) at 2 different molecular weights (MW) (20 and 150 kDa). We collected the eluate at different time points and quantified dextran concentration. We observed significantly improved kinetics with a faster release of dextran with both MW in the iVEP-engineered platform compared to the control empty scaffold (Figures 4C and 4D) (MW 20 kDa min 5 $p < 0.0001$; MW 150 kDa min 4 and 5 $p < 0.0001$). For fluor angiography assay, we infused the PA with 0.2-µm microspheres following a 7-day culture period. Confocal microscopy showed that microspheres remained confined and did not leak into the alveolar space or airways (Figure 4E). This indicates that the formed endothelium is able to preserve tightness and effectively manage the distribution of perfusate within a dynamic 3D organization. Taken together, these findings suggest that iVEPs provide direct perfusion of ViβeSs, owing to their functional integration into the bioengineered vascular framework.

iVEP *in vitro* assessment: Endocrine function and ViβeS survival

After confirmation of spatial integration and perfusion of the bioengineered vascular bed, we assessed the insulin response to glucose stimulation in matured iVEPs compared to ViβeSs on day 7 of culture based on a modified glucose response assay[23] (Figure 5A). When exposed to high glucose (11 mM), matured iVEPs demonstrated significantly higher insulin release compared to ViβeSs (iVEP vs. ViβeSs min 2 $p = 0.0289$; min 3 $p = 0.0205$). Additionally, the peak area under the curve (AUC) for insulin release was notably higher in matured iVEPs than in ViβeSs (AUC: iVEPs: 8.352 ± 1.386 vs. ViβeSs: 5.527 ± 0.4257, $p = 0.0002$, according to Welch's t test; Figure 5B). To assess the capability of iVEP in preserving β cell mass, we monitored β cell mortality over the 7-day maturation period by detecting the presence of miR-375 in the iVEP supernatants, which serves as an indirect marker of β cell death.[24,25] To rule out potential biases from iEC contributions to miR-375 release among various iVEP components, we first assessed miR-375 release in an organ exclusively seeded with iECs (Figure 5C, green line), confirming that endothelial cells do not contribute to miR-375 release in iVEP. Conversely, we observed the kinetics of miR-375 release in the supernatants of iVEP during maturation in the presence of ViβeSs (Figure 5C, cyan line). Of note, by quantifying miR-375 copies in a specific number of cells from each batch, we estimated the percentage of β cell death at various time points (days 0, 1, 3, and 7 of culture, as shown in Figure 5D), allowing us to assess the total β cell loss throughout the maturation of the iVEP organ (Figure 5E). After

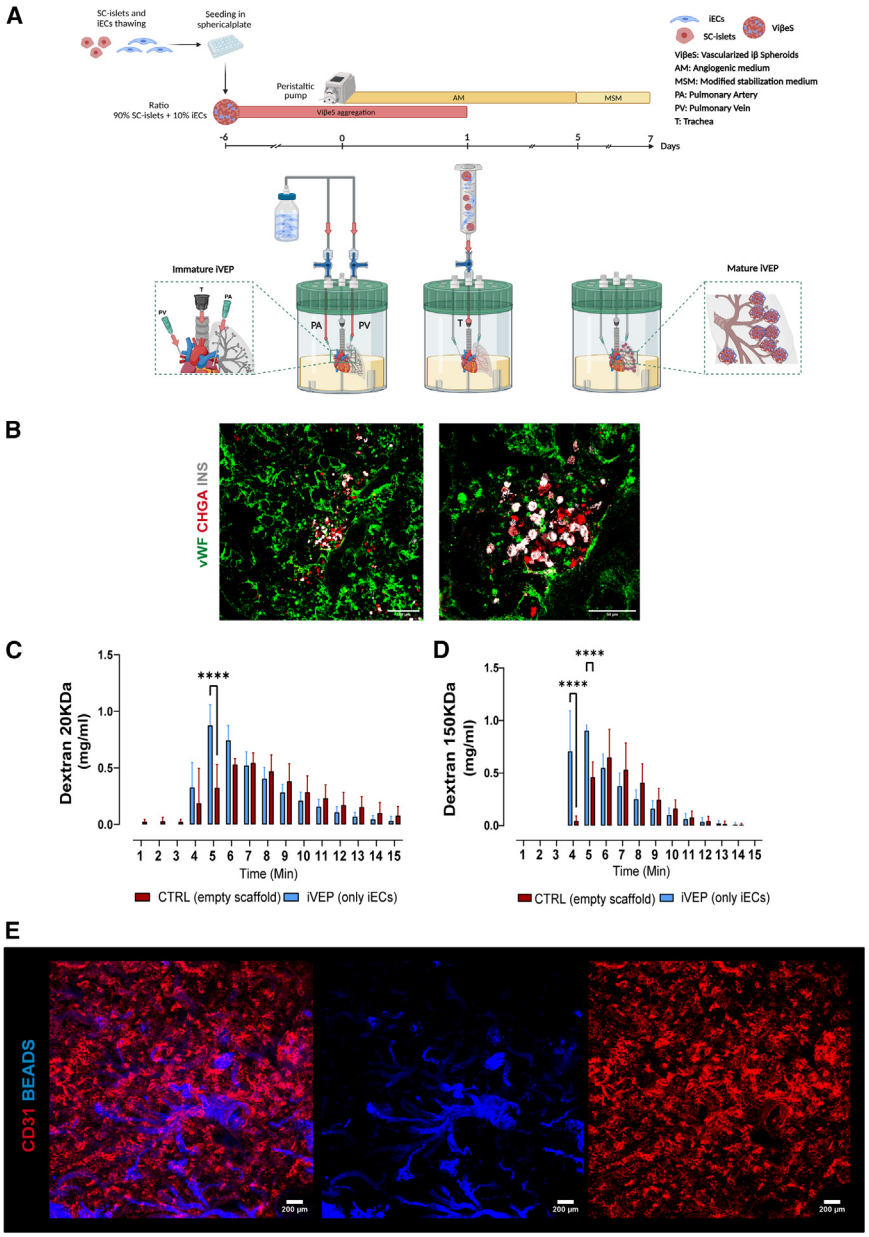

Figure 4. iVEP assembly and *in vitro* functional characterization of vascular compartment

(A) Representative image of iVEP engineering protocol.

(B) Representative image of mature and fully engineered iVEP, with continuous vascular network (human vWF+ in green) and ViβeSs (human CHGA+ in red and human INS+ in gray) fully engrafted and surrounded by iECs.

(C and D) FITC-dextran assay release kinetics. iVEPs were perfused at 1 mL/min with FITC-dextran at two different molecular weights 20 and 150 kDa, respectively. $n = 4$ iVEPs vs. $n = 4$ CTRL empty scaffolds for each MW, $n = 4$ refers to biological replicates.

(E) Fluorescence microsphere perfusion: 0.2-μm microspheres (beads, blue) present and retained in newly formed iVEP vasculature (human CD31, red). Scale bars in μm.

7 days of culture, the SC-islets loss was significantly reduced in the iVEP technology, suggesting an improvement of β cell survival in our platform (percentage of β cell death SC-islets: 62.84% ± 10.38% and iVEP: 14.80% ± 9.11%; Mann-Whitney U test $p = 0.008$) (Figure 5E).

iVEP *in vivo* performance in immunocompromised diabetic mice

Finally, mature iVEPs were tested *in vivo* in a preclinical model of severe diabetes in immune-compromised NSG mice. Diabetes was induced in NSG with a single injection of alloxan (72 mg/kg), and we evaluated graft function over 13 weeks. To optimize integration with the implantation site in the subcutaneous tissue, iVEPs were strategically divided into two segments, and their performance was compared to fresh ViβeSs transplanted into pre-vascularized subcutaneous pouch (DL-ViβeSs) (Figure 6 A). iVEP successfully restored normoglycemia in all transplanted mice within 29 days post transplantation, in contrast to only 2 out of 13 mice (15%) achieving normoglycemia with DL-ViβeS implantation. Notably, the median duration to reach normoglycemia in the iVEP group was 14 ± 1.9 days ($p < 0.0001$, log rank test) (Figure 6C). Additionally, non-fasting glycemia of iVEP-implanted mice was significantly lower compared to DL-ViβeS (DL-ViβeS vs. iVEP $p = 0.00350$; general linear model, repeated measures; Figure 6B). We monitored the graft function quantifying C-pep levels at 1 and 2 weeks after implantation. We noticed significantly improved levels of C-pep in iVEPs vs. DL-ViβeS recipients at both week 1 ($p = 0.0099$, Figure 6D) and week 2 ($p < 0.0001$, Figure 6D). On week 4, an oral glucose tolerance test (OGTT) was performed in all groups. After glucose loading, iVEP recipients showed a significantly lower blood glucose concentration compared to DL-ViβeS recipients (AUC iVEPs vs. DL-ViβeSs $p < 0.0001$ Welch's t test), confirming the superior function of the engrafted scaffold (Figures 6E and 6F). At 4 and 13 weeks of follow-up, the iVEPs were explanted to confirm the graft's contribution to the mice's glucose control. As expected, immediately after iVEP explants, the mice reverted to a diabetic status and displayed hyperglycemia for at least 1 additional week. (Figure 6B, explants#). At the same point, gross pathology evaluation of the explanted iVEPs showed complete integration of the engineered structure in the subcutaneous space, with vessels visibly present in the iVEP structure

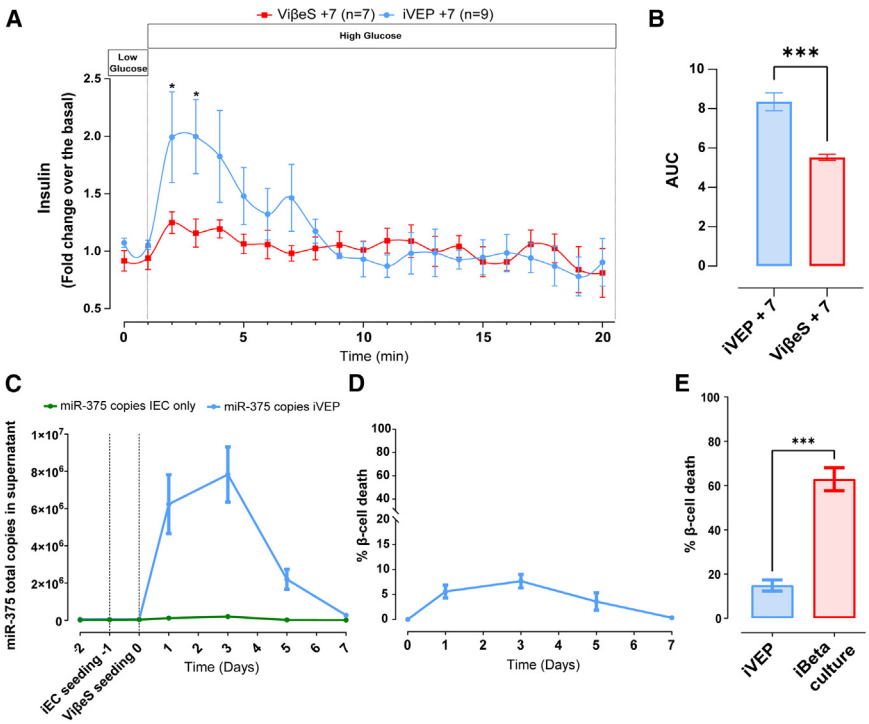

Figure 5. *In vitro* functional evaluation of iVEP endocrine compartment: insulin secretion performance and ViβeS survival

(A) Dynamic insulin secretion test of iVEP (cyan line, $n = 9$ biological replicates) vs. batch-matched ViβeSs (red line, $n = 7$ biological replicates) after 7 days of dynamic culture with low (0.5 mM) and high (11 mM) glucose stimuli. Values are expressed as fold change over the basal (iVEP vs. ViβeS Mann-Whitney U test). Values are presented as mean ± SEM.

(B) Area under the curve (AUC) analysis of insulin secretion test from min 2 to 7. Analysis of iVEPs ($n = 9$ biological replicates) and ViβeS ($n = 7$ biological replicates) performance. AUC peak iVEP vs. ViβeS Welch t test; values are presented as mean ± SEM.

(C) Released miR-375 kinetics (absolute copies in supernatant) during 7 days of culture of mature iVEPs (cyan, $n = 13$ biological replicates) and iVEPs seeded with iECs only (green, $n = 2$ biological replicates). Values are presented as mean ± SEM.

(D) Percentage of β cell death quantified during the 7 days of iVEP maturation culture ($n = 13$ biological replicates). Values are presented as mean ± SD.

(E) Percentage of overall β cell death during the 7 days maturation of iVEPs (cyan, $n = 13$ biological replicates) vs. SC-islets in standard culture (red, $n = 4$ biological replicates). Values are presented as mean ± SEM, $p = 0.0008$, Mann-Whitney U test.

(Figure 7A). Using AngioTool software for quantification, we measured the surface vessel density of the explanted grafts and found an average vessel surface density of 17.38% ± 5.46% across 11 explants, consistent with findings from our previous study (Figure 7B).[22] Immunofluorescence staining confirmed the presence and engraftment of ViβeSs (CHGA+/INS+) within the graft (Figure 7C, left panel). To dissect the specific role of iECs in the engraftment process, iVEPs were engineered in the absence of iEC (iVEPsiECs−). iVEPsiECs− were transplanted in diabetic NSG mice (Figure S5). Results showed that the absence of iECs negatively impacts the time of normoglycemia (Figure S5), suggesting that the presence of endothelial cells represents a key factor in enabling ViβeS engraftment. Additionally, vessel staining was positive for human vWF (Figure 7C, right panel) and mouse CD31 (Figures S6 and S7A), indicating the survival of iEC up to 4 weeks post transplantation and their integration with the host's vasculature. To further demonstrate *in vivo* functional vasculature, 13 weeks after transplantation, an intravascular FITC-dextran perfusion was performed before sample collection. As demonstrated by immunofluorescence staining, iVEP presented endocrine cells (INS+; C-pep+, CHGA+) and dextran-positive vessel structures certifying the graft integration with the host's vasculature (Figure 7C). Notably, after 13 weeks of transplantation, positive vessels for human vWF and FITC dextran were detected (Figure S7B).

DISCUSSION

Organ decellularization is an emerging field, in regenerative medicine, and an attractive technology to produce acellular ECM scaffolds[16] ready for regeneration to finally meet the organ demand for replacement therapy.[26] It was also applied in the T1D field, decellularizing pancreata of rodents,[27,28] porcine,[29] and human[21] origin to generate insulin-producing endocrine tissues for β cell replacement purpose.[30] The final aim was to provide β cell ECM-specific cues to promote their survival and function.[31] These attempts pointed out, for a future clinical application, intrinsic limitations linked to the pancreatic compartment architecture not designed to host more than 5% of the endocrine cells, as well as the need of appropriate cell sources and the generation of functional vascular network for "quick connection" to the recipient's vasculature. Previously, we started to overcome these limitations by repurposing a lung scaffold to a VEP[22,23] using blood outgrowth endothelial cells and immature NPIs as eligible endothelial and insulin-producing cell sources. Immature NPIs in a vascularized ECM architecture showed an improved endocrine functional maturation *in vitro* and immediate function upon transplantation[22] *in vivo*. Stem cell-derived endothelial and β cells represent a relevant, potentially autologous, and endless source of vascular and insulin-producing cells, respectively. As of now, several optimized differentiation protocols are available for both cell types, working on 2D,[10,32,33] in 3D culture, or in a mixed-mode setting,[7,34–36] or exploiting modified mRNAs.[8] The latter can commit iPSC lines, both from healthy and diabetic donor subjects,[6,32,37] to endothelial-like and β-like phenotype similarly resembling an adult native endothelial and β cell, respectively. iECs, at the end of the differentiation protocol, express classical markers of endothelial cells such as CD31 and CD144, exhibiting cobblestone morphology, forming 3D networks on Matrigel, and responding to inflammatory stimuli.[38] iPSC-derived β cells, during differentiation, acquire a more

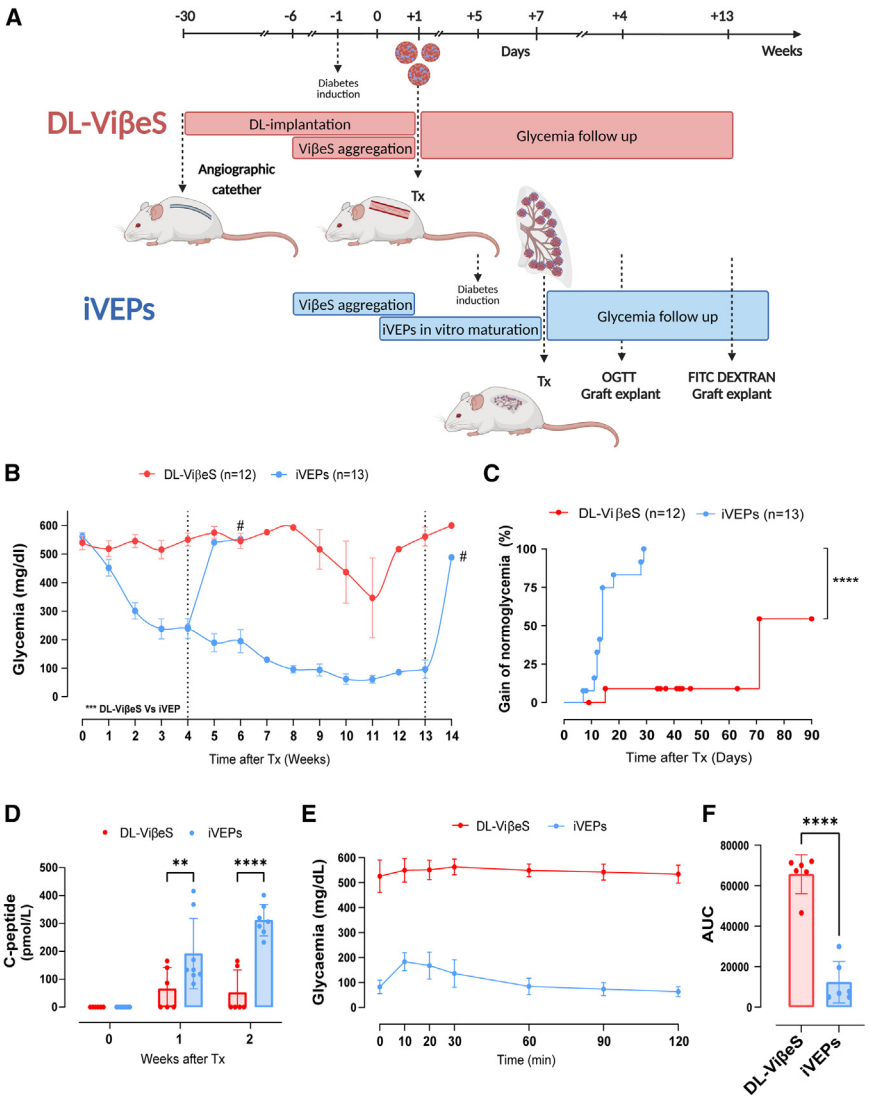

Figure 6. iVEP *in vivo* endocrine performance

(A) Schematic representation of *in vivo* experimental plan for iVEP transplantation in immunocompromised diabetic mouse models.

(B) Daily not fasting glycemia profile comparison between DL-ViβeSs (red, n = 12 recipients) and iVEPs (cyan, n = 13 recipients) for 13 weeks of follow-up (# represent iVEP explant at 4 and 13 weeks, n = 1 explant, respectively). Values are presented as mean ± SEM. DL-ViβeSs vs. iVEPs p = 0.0035, general linear model, repeated measures.

(C) Kaplan-Meier analysis of the percentage of mice reaching normoglycemia (three consecutive measurements ≤200 mg/dL). Differences between iVEPs and DL-ViβeSs were estimated by log rank test ****$p < 0.0001$. Median time to reach normoglycemia iVEP 14 ± 1.9 days

(D) C-peptide quantification at 0, 7, and 14 days after transplantation in iVEP and DL-ViβeS graft bearing recipients. Day 7: DL-ViβeSs (red, n = 6 recipients) vs. iVEPs (cyan, n = 8 recipients) **p = 0.0099. Day 14: DL-ViβeSs (red, n = 6 recipients) vs. iVEPs (cyan, n = 7 recipients) ****$p < 0.0001$. Differences between iVEPs and DL-ViβeS were estimated by two-way ANOVA analysis. Values are presented as mean ± SD.

(E) OGTT of iVEPs and DL-ViβeS recipients at 4 weeks after transplantation. iVEPs (n = 6) vs. DL-ViβeS (n = 6) recipients. Values are presented as mean ± SEM.

(F) AUC quantification of glycemia profile after OGTT. iVEPs (n = 6) vs. DL-ViβeS (n = 6) recipients. Welch's t test ****$p < 0.0001$. Values are presented as mean ± SEM.

mature secretory phenotype, but an *in vivo* maturation step is still required to reach a secretory phenotype partially resembling a native primary β cell, as recently shown using strand-specific RNA sequencing.[39,40] ECM and vasculature microenvironment could be beneficial to the proper functional phenotype maturation of SC-islet cells, their engraftment, and immediate function *in vivo*. Here, we prototyped an innovative iPSC-based scaffold namely iVEP. Indeed, it represents a fully iPSC-based bioengineered device that offers native vascularized organ ECM to ViβeSs, able to conjugate a controlled engraftment *in vitro* coupled with an increased functional performance both *in vitro* and *in vivo*. We engineered iVEP as a proof of concept, with a future aim, to engineer a totally self and clinically compatible platform, based on autologous SC-islets and iEC differentiated from the same subject. In this study, we used commercially available differentiated SC-islets and iECs, already tested in organ and vascular tissue engineering, showing their potential biocompatibility with decellularized matrix for the generation of vascular fluidic devices.[41,42] iECs have a high proliferative capacity and can promote neovascularization *in vivo*,[8] suggesting that they can be directly involved in vessel formation. Firstly, we assessed the compatibility of both iEC and SC-islet phenotype in both standard and iVEP culture media conditions. iECs preserved their phenotype and demonstrated similar behavior in terms of proliferation rate and function in culture, while SC-islets showed the preservation of the endocrine markers and a significant reduction of their survival within 7 days of culture, confirming their committed β cell identity. iECs and SC-islets were then aggregated into ViβeSs for 7 days, showing a stable endothelial composition within the spheroid generation, and used to engineer iVEPs in a two-phase seeding protocol. At day 0, we seeded iECs through the vascular compartment. Then, we seeded a suspension of ViβeSs and iECs through the air compartment of the lung scaffold. By using this two-phase protocol, we can engineer the vascular compartment *in vitro*, pre-vascularizing the site and immediately providing ECM and vascular support to ViβeSs. After an *in vitro* maturation phase of 7 days, the vascular compartment is fully engineered and functional, as revealed by dextran assay and the retention of fluorescent beads (fluo-beads) upon infusion, in line with other lung scaffold-based platforms.[20,22] Thus, the generated vascular network can efficiently be perfused and distribute oxygenated nutrient supply in a 3D structure. The combination of

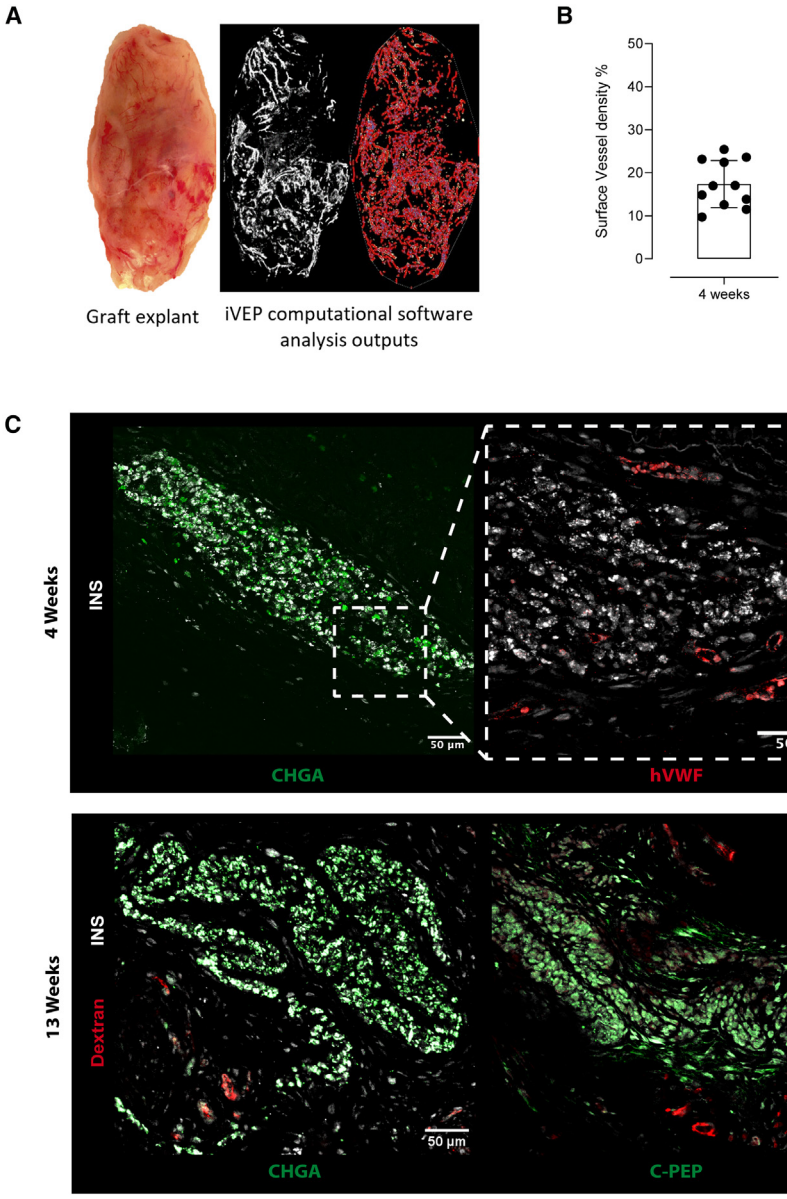

Figure 7. *Ex vivo* iVEP characterization

(A) Gross pathology of 4-week iVEP explants (left) and its computational software analysis of vascular iVEP surface density (middle-right).

(B) Percentage of iVEP surface vessel density at 4 weeks after implantation. Values are presented as mean ± SD; average vessel surface density (17.38 ± 5.46), (n = 11 explants).

(C) Representative IF staining of explanted graft at 4 and 13 weeks after transplantation. Top: left image: ViβeSs (human CHGA+ in green and human INS+ in gray). Right image: ViβeSs (human INS+ in gray) and iECs (human vWF+ in red). Bottom: left image: dextran in red, ViβeSs (human CHGA+ in green and human INS+ in gray). Right image: dextran in red, ViβeSs (human C-pep+ in green and human INS+ in gray).

the ViβeSs (CHGA+/INS+/vWF+ cells) (endocrine compartment) fully integrated with the scaffold-vascularized ECM (vWF+) recreated the physiological endocrine niche microenvironment.[31] In this *in vitro* context, we hypothesized that SC-islets, in close contact with endothelial cells and ECM, receive specific cues that foster their functional activity. To confirm that, we further investigated the endocrine performance of iVEPs vs. batch-matched ViβeSs cultured in standard condition, to assess the contribution of ECM and vasculature microenvironment. As reported by dynamic insulin secretion test, when exposed to high-glucose stimuli, iVEPs responded with a significantly improved insulin release, while batch-matched ViβeSs did not respond in an orchestrated manner, further underlining that SC-islets, within iVEP, acquire a more mature secretory function. As of now, once pluripotent stem cells reach the status of fully differentiated β cells, they require an extensive *in vitro* culture of at least 20 days to finally acquire an orchestrated insulin secretion mechanism in response to stimuli and reach a mature secretory phenotype.[43] We believe that our platform can speed up this process, boosting in differentiated β cells the acquisition of a mature secretory phenotype within 7 days of culture. In addition, concordant literature results demonstrated that the interactions of SC-islets with ECM can affect cell fate specification, promoting a fully committed phenotype.[10] To date, there are very few reports on bioartificial pancreas engineered with SC-islets, endothelial cells, and ECM-based scaffolds, which could be compared with iVEP. Of note, decellularized liver and pancreas scaffolds were engineered with human embryonic stem cell (hESC)-derived pancreatic progenitor (PP) aggregates, and after 9 days of long-term *in vitro* culture, hESC-PPs showed a fully committed endocrine fate[44] suggesting the key role of the matrix into fully committing SC and promoting a phenotype maturation. Also, fully differentiated SC-islets aggregated showed an improved stimulus-dependent Ca^{2+} influx (hallmark of β-cell function)[45] when cultured with endothelial cells in a microfluidic device or improved glucose-mediated insulin secretion when cultured in combination with both primary endothelial cells and Matrigel[46] in static condition; however, no physiologic response to stimuli has been shown, nor functional integration of SC-islets and endothelial cells. In iVEP technology, we are able to architecturally combine vascularized ECM to the endocrine vascularized spheroids and organ dynamic perfusion, suggesting that the combination of these three factors, in the absence of *in vivo* external factor, may foster the SC-islets endocrine function. Another critical point for the *in vitro* biofabrication of insulin-producing tissue is the survival of the β cell mass. Quantifying miR-375, as a marker of β cell death,[47,48]

we demonstrated the ability of iVEP technology to efficiently preserve β cell mass *in vitro*. Finally, we tested iVEP *in vivo* in diabetic immunocompromised mouse models. Several SC-islets, at various differentiation stages (pancreatic progenitors or SC-islets), have been transplanted into different sites such as the kidney capsule (KC),[10,49] the subcutaneous layer,[50] the intramuscular site[51] or into the epididymal fat.[52,53] Each transplantation site has peculiar features[54] such as high vascularization, oxygen tension, minimal surgical invasiveness, and easy graft monitoring. SC-islets showed an amelioration of blood glucose level once transplanted into the intramuscular site[51] or into the epididymal fat[52,53] and a late hyperglycemia reversal after transplantation into the KC[55] or the modified subcutaneous space[50] in a preclinical model of chemically induced T1D using multiple low doses of streptozotocin. This model is characterized by slow diabetes progression compared to the alloxan-induced model characterized by a single high-dose injection of the diabetogenic compound[56] and acute, severe diabetes progression.[56] Thus, considering all the transplantation sites available and looking to a clinical translation of our platform, we decided to transplant iVEP into the subcutaneous space since the site has already been tested in ongoing clinical trials (NCT03163511) as an eligible site due to the possibility to safely radiologically monitor the graft or remove it in case of need. As already reported, the subcutaneous space, per se, has an avascular nature and is considered a less vascularized site compared to others like the kidney or intramuscular one, and it usually requires biomaterials, devices, or a trophic factor to induce early angiogenesis.[57] However, it has already been demonstrated that it is feasible to modify the subcutaneous space using a biomedical-grade nylon catheter able to induce pre-vascularization *in vivo*.[58] The DL strategy has already been tested with both syngeneic murine islets[58] and endoderm progenitors[50] directly transplanted subcutaneously in the pre-vascularized pouch, and both cell sources lead to a late hyperglycemia reversal and preserved function in the follow-up.[50,58] Thus, we compared an *in vivo* pre-vascularized model with our *in vitro* pre-vascularized platform. We transplanted iVEP in the subcutaneous unmodified site and compared its function with batch-matched ViβeSs infused in the modified pre-vascularized subcutaneous space as control. During the *in vivo* follow-up, we noticed a significant improved function in iVEP-transplanted mice, with a median time of 14 days to gain normoglycemia, with a significant amelioration in daily blood glucose levels compared to control group. Thus, we compared an *in vitro* with an *in vivo* pre-vascularization and engraftment, and we demonstrated that *in vitro* engraftment in a pre-vascularized site is faster and more efficient in restoring normoglycemia compared to the *in vivo* counterpart. Additionally, results showed that the absence of iEC significantly negatively impacts the gaining of normoglycemia, suggesting that the presence of endothelial cells represents a key factor in enabling ViβeS engraftment in iVEP. The iVEP platform has demonstrated effectiveness in reducing β cell loss and improving engraftment, which could significantly lower the required dose of SC-derived islets for clinical use. Although the iVEP engineering process is more complex than other technologies currently being tested in clinical trials (NCT03163511, NCT04786262, and NCT05791201), it holds promise for further development as an advanced therapeutic medicinal product.[59] The clinical translation is feasible after solving issues related to scalability and production. Currently, the iVEP platform uses ECM lung scaffold obtained from rats, an inherently incompatible donor source for human application. Furthermore, the small size of the scaffold limits its capacity to host the high cell doses required for human treatment. To overcome these limitations, scaling up the platform and identifying compatible donor sources are essential. In this direction, porcine-derived ECM scaffolds offer a promising alternative, as they are already used in clinical applications, such as porcine pericardium and skin, which serve as compatible substitutes in humans (NCT00958230; NCT06170008). In addition to scaling the bioreactors and devices, standardizing the production of scaffolds and cells under Good Manufacturing Practice (GMP) is critical. Recently, decellularized porcine ECM organs/tissues are on the road to evolve in GMP-compliant production methods. Additionally, SC-islets have been tested in large-scale production at reaching the dose range necessary for treating patients with T1D (NCT04786262).

Limitations of the study

In conclusion, we generated an iVEP, in which SC-islets cells were functionally vascularized and engrafted *in vitro* in a decellularized native organ ECM, which allows an improved endocrine function and a better performance *in vivo*. In the present manuscript, we do not consider the application of the iVEP in an immunocompetent transplantation model to evaluate (1) its function in allogeneic setting and (2) potential immunological mechanisms. Considering the advances in gene editing to engineer hypo-immune cells,[60–63] the use of clinically approved decellularized scaffolds, and the availability of novel strategies for the functionalization of matrix-based scaffolds,[64] in the next future, we plan to manufacture a totally self and clinical-grade platform, able to escape not only allo- but also auto-immune reaction of the graft in the context of T1D.

RESOURCE AVAILABILITY

Lead contact

Further information and requests for resources and reagents should be directed to the lead contact, Dr. Antonio Citro (citro.antonio@hsr.it).

Materials availability

Reagents are available upon request to the lead contact.

Data and code availability

- Data collected and presented in this work will be made available by reasonable request to the corresponding author.
- There is no code to report.
- Any raw data and information required to reanalyze data reported in this work are available from the lead contact upon request.

ACKNOWLEDGMENTS

This study was supported by a seed grant from Ospedale San Raffaele. The authors thank Paola Macchieraldo, Antonio Mincione, Elena Riva, Antonio Civita, Andrea Marchesi, and Michele Mainardi for supporting the fundraising campaign "Un brutto t1po." We thank Matteo Monieri for the technical contribution in *in vivo* mouse experiments. Immunofluorescence acquisition was carried out in the San Raffaele Scientific Institute ALEMBIC facility. Sample embedding and slides preparation were carried out in San Raffaele Scientific Institute Animal histopathology facility. All the cartoon figures were created with BioRender. The present work was performed by F.C. in partial fulfillment

of the requirements for obtaining the PhD degree at Vita-Salute San Raffaele University, Milano, Italy. Work performed by A.N. was in partial fulfillment of the requirements for obtaining the PhD degree at Vita-Salute San Raffaele University, Milano, Italy.

AUTHOR CONTRIBUTIONS

F.C. conducted and analyzed all the experiments and contributed to manuscript preparation. A.N. assisted with immunofluorescence (IF) and flow cytometry staining and contributed to the manuscript preparation. C.P. assisted with organ engineering. L.V. contributed to insulin secretion testing. S.P. helped with iPSC-derived β cell flow cytometry and *in vivo* experiments. F.M. assisted with vascular reconstruction immunofluorescence. I.M. and V.L. helped with miRNA extraction, quantification, and analysis. L.P. contributed with manuscript preparation. A.C. conceptualized the study design, oversaw the experimental conduction and data analysis, and is responsible for the manuscript.

DECLARATION OF INTERESTS

The authors declare no competing interests.

STAR★METHODS

Detailed methods are provided in the online version of this paper and include the following:

- KEY RESOURCES TABLE
- EXPERIMENTAL MODEL AND STUDY PARTICIPANT DETAILS
  - Rats and mice
  - Cell lines
- METHOD DETAILS
  - Preparation of acellular lung scaffolds
  - Incucyte proliferation assay
  - Tube formation assay
  - Dynamic insulin secretion test (IST) of ViβeS
  - *In vitro* seeding and culture of iVEPs
  - *In vitro* FITC-Dextran assay
  - Fluorescence microangiography
  - Dynamic insulin secretion tests (IST) of iVEPs
  - miR-375 analysis and quantification
  - Diabetes induction and metabolic monitoring
  - Device-less subcutaneous transplant site generation and ViβeS transplantation
  - iVEPs implantations in diabetic recipient mice
  - Oral glucose tolerance test
  - iVEPs vessel density and dextran assay
  - Flow cytometry
  - Histology and immunostaining
- QUANTIFICATION AND STATISTICAL ANALYSIS

SUPPLEMENTAL INFORMATION

Supplemental information can be found online at https://doi.org/10.1016/j.xcrm.2025.101938.

Received: March 15, 2024
Revised: November 18, 2024
Accepted: January 13, 2025
Published: February 7, 2025

REFERENCES

1. Gregory, G.A., Robinson, T.I.G., Linklater, S.E., Wang, F., Colagiuri, S., de Beaufort, C., Donaghue, K.C., International Diabetes Federation Diabetes Atlas Type 1 Diabetes in Adults Special Interest Group; Magliano, D.J., and Maniam, J. (2022). Global incidence, prevalence, and mortality of type 1 diabetes in 2021 with projection to 2040: a modelling study. Lancet Diabetes Endocrinol. *10*, 741–760.
2. Beck, R.W., Bergenstal, R.M., Laffel, L.M., and Pickup, J.C. (2019). Advances in technology for management of type 1 diabetes. Lancet *394*, 1265–1273.
3. Piemonti, L. (2021). Felix dies natalis, insulin, ceterum autem censeo 'beta is better. Acta Diabetol. *58*, 1287–1306.
4. Pepper, A.R., Bruni, A., and Shapiro, A.M.J. (2018). Clinical islet transplantation: Is the future finally now? Curr. Opin. Organ Transplant. *23*, 428–439, Preprint at. https://doi.org/10.1097/MOT.0000000000000546.
5. Pagliuca, F.W., Millman, J.R., Gürtler, M., Segel, M., Van Dervort, A., Ryu, J.H., Peterson, Q.P., Greiner, D., and Melton, D.A. (2014). Generation of functional human pancreatic β cells in vitro. Cell *159*, 428–439.
6. Millman, J.R., Xie, C., Van Dervort, A., Gürtler, M., Pagliuca, F.W., and Melton, D.A. (2016). Generation of stem cell-derived beta-cells from patients with type 1 diabetes. Nat. Commun. *7*, 11463.
7. Barsby, T., Ibrahim, H., Lithovius, V., Montaser, H., Balboa, D., Vähäkangas, E., Chandra, V., Saarimäki-Vire, J., and Otonkoski, T. (2022). Differentiating functional human islet-like aggregates from pluripotent stem cells. STAR Protoc. *3*, 101711.
8. Wang, K., Lin, R.Z., Hong, X., Ng, A.H., Lee, C.N., Neumeyer, J., Wang, G., Wang, X., Ma, M., Pu, W.T., et al. (2020). Robust differentiation of human pluripotent stem cells into endothelial cells via temporal modulation of ETV2 with modified mRNA. Sci. Adv. *6*, eaba7606.
9. Nguyen, J., Lin, Y.Y., and Gerecht, S. (2021). The next generation of endothelial differentiation: Tissue-specific ECs. Cell Stem Cell *28*, 1188–1204.
10. Hogrebe, N.J., Augsornworawat, P., Maxwell, K.G., Velazco-Cruz, L., and Millman, J.R. (2020). Targeting the cytoskeleton to direct pancreatic differentiation of human pluripotent stem cells. Nat. Biotechnol. *38*, 460–470. https://doi.org/10.1038/s41587-020-0430-6.
11. Dupont, S., Morsut, L., Aragona, M., Enzo, E., Giulitti, S., Cordenonsi, M., Zanconato, F., Le Digabel, J., Forcato, M., Bicciato, S., et al. (2011). Role of YAP/TAZ in mechanotransduction. Nature *474*, 179–183.
12. Swift, J., Ivanovska, I.L., Buxboim, A., Harada, T., Dingal, P.C.D.P., Pinter, J., Pajerowski, J.D., Spinler, K.R., Shin, J.W., Tewari, M., et al. (2013). Nuclear lamin-A scales with tissue stiffness and enhances matrix-directed differentiation. Science *341*, 341.
13. Berger, C., Bjørlykke, Y., Hahn, L., Mühlemann, M., Kress, S., Walles, H., Luxenhofer, R., Ræder, H., Metzger, M., and Zdzieblo, D. (2020). Matrix decoded - A pancreatic extracellular matrix with organ specific cues guiding human iPSC differentiation. Biomaterials *244*, 119766.
14. Shapiro, A.M.J., Thompson, D., Donner, T.W., Bellin, M.D., Hsueh, W., Pettus, J., Wilensky, J., Daniels, M., Wang, R.M., Brandon, E.P., et al. (2021). Insulin expression and C-peptide in type 1 diabetes subjects implanted with stem cell-derived pancreatic endoderm cells in an encapsulation device. Cell Rep. Med. *2*, 100466.
15. Keymeulen, B., De Groot, K., Jacobs-Tulleneers-Thevissen, D., Thompson, D.M., Bellin, M.D., Kroon, E.J., Daniels, M., Wang, R., Jaiman, M., Kieffer, T.J., et al. (2024). Encapsulated stem cell – derived β cells exert glucose control in patients with type 1 diabetes. Nat. Biotechnol. *42*, 1507–1514. https://doi.org/10.1038/s41587-023-02055-5.
16. Guyette, J.P., Gilpin, S.E., Charest, J.M., Tapias, L.F., Ren, X., and Ott, H.C. (2014). Perfusion decellularization of whole organs. Nat. Protoc. *9*, 1451–1468.
17. Ott, H.C., Matthiesen, T.S., Goh, S.K., Black, L.D., Kren, S.M., Netoff, T.I., and Taylor, D.A. (2008). Perfusion-decellularized matrix: Using nature's platform to engineer a bioartificial heart. Nat. Med. *14*, 213–221.
18. Song, J.J., Guyette, J.P., Gilpin, S.E., Gonzalez, G., Vacanti, J.P., and Ott, H.C. (2013). Regeneration and experimental orthotopic transplantation of a bioengineered kidney. Nat. Med. *19*, 646–651.
19. Ott, H.C., Clippinger, B., Conrad, C., Schuetz, C., Pomerantseva, I., Ikonomou, L., Kotton, D., and Vacanti, J.P. (2010). Regeneration and orthotopic transplantation of a bioartificial lung. Nat. Med. *16*, 927–933.

20. Ren, X., Moser, P.T., Gilpin, S.E., Okamoto, T., Wu, T., Tapias, L.F., Mercier, F.E., Xiong, L., Ghawi, R., Scadden, D.T., et al. (2015). Engineering pulmonary vasculature in decellularized rat and human lungs. Nat. Biotechnol. *33*, 1097–1102.

21. Peloso, A., Urbani, L., Cravedi, P., Katari, R., Maghsoudlou, P., Fallas, M.E.A., Sordi, V., Citro, A., Purroy, C., Niu, G., et al. (2016). The Human Pancreas as a Source of Pro-Tolerogenic Extracellular Matrix Scaffold for a New Generation Bio-Artificial Endocrine Pancreas. Ann. Surg. *264*, 169–179.

22. Citro, A., Neroni, A., Pignatelli, C., Campo, F., Policardi, M., Monieri, M., Pellegrini, S., Dugnani, E., Manenti, F., Maffia, M.C., et al. (2023). Directed self-assembly of a xenogeneic vascularized endocrine pancreas for type 1 diabetes. Nat. Commun. *14*, 878.

23. Citro, A., Moser, P.T., Dugnani, E., Rajab, T.K., Ren, X., Evangelista-Leite, D., Charest, J.M., Peloso, A., Podesser, B.K., Manenti, F., et al. (2019). Biofabrication of a vascularized islet organ for type 1 diabetes. Biomaterials *199*, 40–51.

24. Erener, S., Mojibian, M., Fox, J.K., Denroche, H.C., and Kieffer, T.J. (2013). Circulating miR-375 as a biomarker of β-cell death and diabetes in mice. Endocrinology *154*, 603–608.

25. Poy, M.N., Eliasson, L., Krutzfeldt, J., Kuwajima, S., Ma, X., Macdonald, P.E., Pfeffer, S., Tuschl, T., Rajewsky, N., Rorsman, P., and Stoffel, M. (2004). A pancreatic islet-specific microRNA regulates insulin secretion. Nature *432*, 226–230.

26. Abouna, G.M. (2008). Organ Shortage Crisis: Problems and Possible Solutions. Transplant. Proc. *40*, 34–38.

27. Goh, S.K., Bertera, S., Olsen, P., Candiello, J.E., Halfter, W., Uechi, G., Balasubramani, M., Johnson, S.A., Sicari, B.M., Kollar, E., et al. (2013). Perfusion-decellularized pancreas as a natural 3D scaffold for pancreatic tissue and whole organ engineering. Biomaterials *34*, 6760–6772.

28. Napierala, H., Hillebrandt, K.H., Haep, N., Tang, P., Tintemann, M., Gassner, J., Noesser, M., Everwien, H., Seiffert, N., Kluge, M., et al. (2017). Engineering an endocrine Neo-Pancreas by repopulation of a decellularized rat pancreas with islets of Langerhans. Sci. Rep. *7*, 41777.

29. Mirmalek-Sani, S.-H., Orlando, G., McQuilling, J.P., Pareta, R., Mack, D.L., Salvatori, M., Farney, A.C., Stratta, R.J., Atala, A., Opara, E.C., and Soker, S. (2014). Porcine pancreas extracellular matrix as a platform for endocrine pancreas bioengineering. Biomaterials *34*, 5488–5495.

30. Campo, F., Neroni, A., Pignatelli, C., Bignard, J., Berishvili, E., Piemonti, L., and Citro, A. (2023). In Bioengineered Vascularized Insulin Producing Endocrine Tissues BT - Pluripotent Stem Cell Therapy for Diabetes, L. Piemonti, J. Odorico, T.J. Kieffer, V. Sordi, and E. de Koning, eds. (Cham: Springer International Publishing), pp. 151–177. https://doi.org/10.1007/978-3-031-41943-0_8.

31. Pignatelli, C., Campo, F., Neroni, A., Piemonti, L., and Citro, A. (2022). Bioengineering the Vascularized Endocrine Pancreas: A Fine-Tuned Interplay Between Vascularization, Extracellular-Matrix-Based Scaffold Architecture, and Insulin-Producing Cells. Transpl. Int. *35*, 10555.

32. Samuel, R., Daheron, L., Liao, S., Vardam, T., Kamoun, W.S., Batista, A., Buecker, C., Schäfer, R., Han, X., Au, P., et al. (2013). Generation of functionally competent and durable engineered blood vessels from human induced pluripotent stem cells. Proc. Natl. Acad. Sci. USA *110*, 12774–12779.

33. Wang, L., Xiang, M., Liu, Y., Sun, N., Lu, M., Shi, Y., Wang, X., Meng, D., Chen, S., and Qin, J. (2016). Human induced pluripotent stem cells derived endothelial cells mimicking vascular inflammatory response under flow. Biomicrofluidics *10*, 014106.

34. Zhang, S., Dutton, J.R., Su, L., Zhang, J., and Ye, L. (2014). The influence of a spatiotemporal 3D environment on endothelial cell differentiation of human induced pluripotent stem cells. Biomaterials *35*, 3786–3793.

35. Talavera-Adame, D., Wu, G., He, Y., Ng, T.T., Gupta, A., Kurtovic, S., Hwang, J.Y., Farkas, D.L., and Dafoe, D.C. (2011). Endothelial cells in co-culture enhance embryonic stem cell differentiation to pancreatic progenitors and insulin-producing cells through BMP signaling. Stem Cell Rev. Rep. *7*, 532–543.

36. Millman, J.R., and Pagliuca, F.W. (2017). Autologous pluripotent stem cell-derived β-like cells for diabetes cellular therapy. Diabetes *66*, 1111–1120.

37. Hogrebe, N.J., Maxwell, K.G., Augsornworawat, P., and Millman, J.R. (2021). Generation of insulin-producing pancreatic β cells from multiple human stem cell lines. Nat. Protoc. *16*, 4109–4143.

38. Jang, S., Collin de l'Hortet, A., and Soto-Gutierrez, A. (2019). Induced Pluripotent Stem Cell–Derived Endothelial Cells: Overview, Current Advances, Applications, and Future Directions. Am. J. Pathol. *189*, 502–512.

39. Balboa, D., Barsby, T., Lithovius, V., Saarimäki-Vire, J., Omar-Hmeadi, M., Dyachok, O., Montaser, H., Lund, P.E., Yang, M., Ibrahim, H., et al. (2022). Functional, metabolic and transcriptional maturation of human pancreatic islets derived from stem cells. Nat. Biotechnol. *40*, 1042–1055.

40. Augsornworawat, P., Hogrebe, N.J., Ishahak, M., Schmidt, M.D., Marquez, E., Maestas, M.M., Veronese-Paniagua, D.A., Gale, S.E., Miller, J.R., Velazco-Cruz, L., and Millman, J.R. (2023). Single-nucleus multiomics of human stem cell-derived islets identifies deficiencies in lineage specification. Nat. Cell Biol. *25*, 904–916.

41. Belair, D.G., Whisler, J.A., Valdez, J., Velazquez, J., Molenda, J.A., Vickerman, V., Lewis, R., Daigh, C., Hansen, T.D., Mann, D.A., et al. (2015). Human vascular tissue models formed from human induced pluripotent stem cell derived endothelial cells. Stem Cell Rev. Rep. *11*, 511–525.

42. Caralt, M., Uzarski, J.S., Iacob, S., Obergfell, K.P., Berg, N., Bijonowski, B.M., Kiefer, K.M., Ward, H.H., Wandinger-Ness, A., Miller, W.M., et al. (2015). Optimization and critical evaluation of decellularization strategies to develop renal extracellular matrix scaffolds as biological templates for organ engineering and transplantation. Am. J. Transplant. *15*, 64–75.

43. Velazco-Cruz, L., Song, J., Maxwell, K.G., Goedegebuure, M.M., Augsornworawat, P., Hogrebe, N.J., and Millman, J.R. (2019). Acquisition of Dynamic Function in Human Stem Cell-Derived β Cells. Stem Cell Rep. *12*, 351–365.

44. Goh, S.K., Bertera, S., Richardson, T., and Banerjee, I. (2023). Repopulation of decellularized organ scaffolds with human pluripotent stem cell-derived pancreatic progenitor cells. Biomed. Mater. *18*, 025018.

45. Jun, Y., Nguyen-Ngoc, K.V., Sai, S., Bender, R.H.F., Kravets, V., Zhu, H., Hatch, C.J., Schlichting, M., Gaetani, R., Mallick, M., and Hachey, S.J. (2022). Engineered Vasculature Induces Functional Maturation of Pluripotent Stem Cell- Derived Islet Organoids. bioRxiv *1–47*, 2022.

46. Augsornworawat, P., Velazco-Cruz, L., Song, J., and Millman, J.R. (2019). A hydrogel platform for in vitro three dimensional assembly of human stem cell-derived islet cells and endothelial cells. Acta Biomater. *97*, 272–280.

47. Kanak, M.A., Takita, M., Shahbazov, R., Lawrence, M.C., Chung, W.Y., Dennison, A.R., Levy, M.F., and Naziruddin, B. (2015). Evaluation of MicroRNA375 as a Novel Biomarker for Graft Damage in Clinical Islet Transplantation. Transplantation *99*, 1568–1573.

48. Sims, E.K., Evans-Molina, C., Tersey, S.A., Eizirik, D.L., and Mirmira, R.G. (2018). Biomarkers of islet beta cell stress and death in type 1 diabetes. Diabetologia *61*, 2259–2265.

49. Rezania, A., Bruin, J.E., Arora, P., Rubin, A., Batushansky, I., Asadi, A., O'Dwyer, S., Quiskamp, N., Mojibian, M., Albrecht, T., et al. (2014). Reversal of diabetes with insulin-producing cells derived in vitro from human pluripotent stem cells. Nat. Biotechnol. *32*, 1121–1133.

50. Pepper, A.R., Pawlick, R., Bruni, A., Wink, J., Rafiei, Y., O'Gorman, D., Yan-Do, R., Gala-Lopez, B., Kin, T., MacDonald, P.E., and Shapiro, A.M.J. (2017). Transplantation of Human Pancreatic Endoderm Cells Reverses Diabetes Post Transplantation in a Prevascularized Subcutaneous Site. Stem Cell Rep. *8*, 1689–1700.

51. Maxwell, K.G., Kim, M.H., Gale, S.E., and Millman, J.R. (2022). Differential Function and Maturation of Human Stem Cell-Derived Islets after Transplantation. Stem Cells Transl. Med. *11*, 322–331.

52. Kim, Y., Kim, H., Ko, U.H., Oh, Y., Lim, A., Sohn, J.W., Shin, J.H., Kim, H., and Han, Y.M. (2016). Islet-like organoids derived from human pluripotent

stem cells efficiently function in the glucose responsiveness in vitro and in vivo. Sci. Rep. *6*, 35145.

53. Stock, A.A., Manzoli, V., De Toni, T., Abreu, M.M., Poh, Y.C., Ye, L., Roose, A., Pagliuca, F.W., Thanos, C., Ricordi, C., and Tomei, A.A. (2020). Conformal Coating of Stem Cell-Derived Islets for β Cell Replacement in Type 1 Diabetes. Stem Cell Rep. *14*, 91–104.
54. Cayabyab, F., Nih, L.R., and Yoshihara, E. (2021). Advances in Pancreatic Islet Transplantation Sites for the Treatment of Diabetes. Front. Endocrinol. *12*, 732431, Preprint at. https://doi.org/10.3389/fendo.2021.732431.
55. Pileggi, A., Molano, R.D., Ricordi, C., Zahr, E., Collins, J., Valdes, R., and Inverardi, L. (2006). Reversal of diabetes by pancreatic islet transplantation into a subcutaneous, neovascularized device. Transplantation *81*, 1318–1324.
56. Lenzen, S. (2008). The mechanisms of alloxan- and streptozotocin-induced diabetes. Diabetologia *51*, 216–226.
57. Sakata, N., Aoki, T., Yoshimatsu, G., Tsuchiya, H., Hata, T., Katayose, Y., Egawa, S., and Unno, M. (2014). Strategy for clinical setting in intramuscular and subcutaneous islet transplantation. Diabetes. Metab. Res. Rev. *30*, 1–10.
58. Pepper, A.R., Gala-Lopez, B., Pawlick, R., Merani, S., Kin, T., and Shapiro, A.M.J. (2015). A prevascularized subcutaneous device-less site for islet and cellular transplantation. Nat. Biotechnol. *33*, 518–523.
59. Grattoni, A., Korbutt, G., Tomei, A.A., García, A.J., Pepper, A.R., Stabler, C., Brehm, M., Papas, K., Citro, A., Shirwan, H., et al. (2025). Harnessing cellular therapeutics for type 1 diabetes mellitus: progress, challenges, and the road ahead. Nat. Rev. Endocrinol. *21*, 14–30, Preprint at. https://doi.org/10.1038/s41574-024-01029-0.
60. Chimienti, R., Baccega, T., Torchio, S., Manenti, F., Pellegrini, S., Cospito, A., Amabile, A., Lombardo, M.T., Monti, P., Sordi, V., et al. (2022). Engineering of immune checkpoints B7-H3 and CD155 enhances immune compatibility of MHC-I−/− iPSCs for β cell replacement. Cell Rep. *40*, 111423.
61. Hu, X., White, K., Olroyd, A.G., DeJesus, R., Dominguez, A.A., Dowdle, W.E., Friera, A.M., Young, C., Wells, F., Chu, E.Y., et al. (2024). Hypoimmune induced pluripotent stem cells survive long term in fully immunocompetent, allogeneic rhesus macaques. Nat. Biotechnol. *42*, 413–423. https://doi.org/10.1038/s41587-023-01784-x.
62. Hu, X., Gattis, C., Olroyd, A.G., Friera, A.M., White, K., Young, C., Basco, R., Lamba, M., Wells, F., Ankala, R., et al. (2023). Human hypoimmune primary pancreatic islets avoid rejection and autoimmunity and alleviate diabetes in allogeneic humanized mice. Sci. Transl. Med. *15*, eadg5794.
63. Gerace, D., Zhou, Q., Kenty, J.H.R., Veres, A., Sintov, E., Wang, X., Boulanger, K.R., Li, H., and Melton, D.A. (2023). Engineering human stem cell-derived islets to evade immune rejection and promote localized immune tolerance. Cell Rep. Med. *4*, 100879.
64. Wang, X., Brown, N.K., Wang, B., Shariati, K., Wang, K., Fuchs, S., Melero-Martin, J.M., and Ma, M. (2021). Local Immunomodulatory Strategies to Prevent Allo-Rejection in Transplantation of Insulin-Producing Cells. Adv. Sci. *8*, 1–19.
65. Piemonti, L. (1999). Effects of cryopreservation on in vitro and in vivo long-term function of human islets1. Transplantation *68*, 655–662.
66. Marzinotto, I., Pellegrini, S., Brigatti, C., Nano, R., Melzi, R., Mercalli, A., Liberati, D., Sordi, V., Ferrari, M., Falconi, M., et al. (2017). miR-204 is associated with an endocrine phenotype in human pancreatic islets but does not regulate the insulin mRNA through MAFA. Sci. Rep. *7*, 14051.
67. Berman, D.M., Molano, R.D., Fotino, C., Ulissi, U., Gimeno, J., Mendez, A.J., Kenyon, N.M., Kenyon, N.S., Andrews, D.M., Ricordi, C., and Pileggi, A. (2016). Bioengineering the endocrine pancreas: Intraomental islet transplantation within a biologic resorbable scaffold. Diabetes *65*, 1350–1361.
68. Leiter, E.H., and Schile, A. (2013). Genetic and Pharmacologic Models for Type 1 Diabetes. Curr. Protoc. Mol. Biol. *3*, 9–19.
69. Citro, A., Cantarelli, E., Pellegrini, S., Dugnani, E., and Piemonti, L. (2018). Anti-Inflammatory Strategies in Intrahepatic Islet Transplantation: A Comparative Study in Preclinical Models. Transplantation *102*, 240–248.
70. Zudaire, E., Gambardella, L., Kurcz, C., and Vermeren, S. (2011). A computational tool for quantitative analysis of vascular networks. PLoS One *6*, e27385.

STAR★METHODS

KEY RESOURCES TABLE

REAGENT or RESOURCE	SOURCE	IDENTIFIER
Antibodies		
Anti-human CD31	Dako	Cat# M082301; RRID: AB_2114471
Anti-human CD144	R&D	Cat# AF938; RRID: AB_355726
Anti-human Chromogranin A	Abcam	Cat# A15160; RRID: AB_301704
Anti-human Chromogranin A	Invitrogen	Cat# MA513096; RRID: AB_10987033
Anti-human C-peptide	Abcam	Cat# AB14181 RRID: AB_300968
Anti-human Insulin	Agilent	Cat# IR00261-2; RRID: AB_2800361
Anti-human Nkx6.1	Bio-Techne	Cat# NBP1-49672; RRID: AB_10011794
Anti-human Pdx1	Bio-Techne	Cat# AF2419; RRID: AB_355257
Anti-human Von Willebrand Factor	Dako	Cat# A0082; RRID: AB_2315602
Anti-mouse CD31	Cell Signaling	Cat# 77699S; RRID: AB_2722705
Anti-mouse CD31	BD Pharmingen	Cat# 550274; RRID: AB_393571
Anti-human CD90-APC	R&D Systems	Cat# FAB2067A
Anti-human CD105 FITC	BD Biosciences	Cat# 561443; RRID: AB_10714629
Anti-human CD31 APC-Cy7	BioLegend	Cat# 303119; RRID: AB_10643590
Anti-human CD73 PE	BD Pharmingen	Cat# 550257; RRID: AB_393561
Anti-human INSULIN Alexa Fluor 647	BD Pharmingen	Cat# 565689; RRID: AB_2739331
Anti-human NKX6.1 PE	BD Pharmingen	Cat# 563023; RRID: AB_2716792
Anti-human PDX1 Alexa Fluor 488	BD Pharmingen	Cat# 562274; RRID: AB_10924596
Chemicals, peptides, and recombinant proteins		
5-French (Fr.) textured nylon radiopaque angiographic catheter	Cook Medical, Indiana, USA	Cat# AI-07130-J
Alloxan monohydrate	Sigma	Cat# A7413
Fluorescein isothiocyanate-dextran - 150KDa	Merck	Cat# FD150S
Fluorescein isothiocyanate-dextran - 20KDa	Merck	Cat# FD20S
FluoSpheres (0.2 μm, 365/415)	Invitrogen	Cat# F8805
Kugelmeier Sphericalplate 5Ds	Kugelmeier L.T.D.	N/A
LinBit pellet	LinShin	N/A
Live/Dead Dye	Life Technologies	Cat# 34964
Low melting point agarose	Invitrogen	Cat# 16520050
Matrigel®	Corning®	Cat# 354234
OCT compound	Tissue Tek	Cat# 4583
Sodium Dodecyl Sulfate	Sigma-Aldrich	Cat# L4509
Phosphate Buffered Saline	Corning	Cat# 21040C
Triton X-100	Sigma-Aldrich	Cat# X100
VascuLife® VEGF Endothelial Medium Complete Kit	Lifeline cell technology	Cat# LL-0003
Critical commercial assays		
Human Insulin ELISA Kit	Mercodia	Cat# 10-1113-10
Human C-peptide ELISA Kit	Mercodia	Cat# 10-1136-01
Maxwell® RSC miRNA Plasma and Serum Kit	Promega	Cat# AS1680
NucleoSpin miRNA Plasma kit	Macherey-Nagel, Düren	Cat# 740981.5

(*Continued on next page*)

Continued		
REAGENT or RESOURCE	SOURCE	IDENTIFIER
TaqMan® MicroRNA Reverse Transcription kit	Applied Biosystems	Cat# 4366596
Experimental models: Cell lines		
Cellartis® hiPS Beta Cells (from ChiPSC12)	TAKARA BIO	Y10100
iCell Endothelial Cells, 01434	Fujifilm cellular dynamics	R1022
Experimental models: Organisms/strains		
Rat: Lewis rat	Charles river laboratory	Lewis rat Inbreed
Mouse: NOD.Cg-Prkdc^{scid} Il2rg^{tm1Wjl}/SzJ	Charles river laboratory	Strain #: 005557 RRID: IMSR_JAX:005557
Software and algorithms		
AngioTool 64 version 0.6a	Zudaire et al.[69]	https://ccrod.cancer.gov/confluence/display/ROB2/Home
Graphpad Prism v10	GraphPad Software	http://www.graphpad.com
ImageJ		https://imagej.net/ij/
SPSS v20	IBM	https://www.ibm.com/it-it/products/spss-statistics
Other		
Incucyte®	Sartorius	https://www.sartorius.com/en/products/live-cell-imaging-analysis/live-cell-analysis-instruments
CYTOFLEX S/LX	BECKMAN COULTER	https://www.beckman.com/flow-cytometry/research-flow-cytometers/cytoflex-lx
Confocals Olympus FluoVIEW 3000 RS	Olympus	https://www.olympus-lifescience.com/en/laser-scanning/fv3000/
FACSCantoII	BD Biosciences	https://www.bdbiosciences.com/en-eu/products/instruments/flow-cytometers/clinical-cell-analyzers/facscanto

EXPERIMENTAL MODEL AND STUDY PARTICIPANT DETAILS

Rats and mice

Experiments involving rats and mice were performed under protocols approved and monitored by the Animal Care and Use Committee of San Raffaele Scientific Institute. Male Lewis rats (225-250g; Charles River Laboratories) were used as scaffold donors. Female NSG (NOD.Cg-Prkdcscid Il2rgtm1Wjl/SzJ) immune-compromised mice (24–26 g; Charles River Laboratories, calco, Italy) were used as transplant recipients.

Cell lines

iPSC-derived endothelial cells

Purified human endothelial cells (iEC) derived from iPSCs (Cellular Dynamics International, Inc. Madison, WI) were used for iVEPs generation upon thawing and expansion in standard culture conditions according to product datasheet. iECs were sourced from skin fibroblasts from a healthy Caucasian female volunteer (age <18-years-old). CD31+/CD105+/CD73+/CD90-markers were used to define the endothelial cells phenotype. Only batches of cells with CD31/CD105/CD73 markers >90% and CD90 < 5% at population level were considered eligible for iVEP generation.

iPSC-derived β cells and vascularized iβ spheroid generation (ViβeS) protocol

Mature human β cells derived from iPSCs (SC-islets) (Takara Bio) were used. SC-islets were sourced from skin fibroblasts from a healthy 24-year-old European/North African male volunteer (77 kg/177 cm). After thawing and 7 days of acclimation in the specific culture medium (Cellartis Beta Cell Maintenance Medium), cells were evaluated by flow cytometry to confirm their specific mature phenotype. Pdx1, Nkx 6.1 and Insulin markers were used to define and confirm the endocrine phenotype. Only batches of cells at population level with Pdx1>95%, Nkx6.1 > 20% and Ins>55% were considered eligible for spheroid aggregation and iVEP generation. SC-islets were seeded in Kugelmeier Sphericalplate 5Ds together with iECs (1000 cells per spheroid with the ratio of 90% SC-islets +10% iECs) to generate ViβeS. Spheroids were cultured according to SC-islets culture protocol (standard culture conditions by datasheet provided TAKARA BIO) for 7 days (acclimatation) and then seeded in iVEP.

METHOD DETAILS

Preparation of acellular lung scaffolds

Cadaveric rat lungs were isolated and decellularized by perfusion as previously described.[19] In brief, cadaveric lungs were explanted from male Lewis rats (225–250 g, Charles River Laboratories) after systemic heparinization. The pulmonary artery (PA) was cannulated with a 18G cannula (McMaster-Carr), the pulmonary veins (PV) were cannulated through the left atrial appendage using a miniball cannula with tip basket (1.9 mm ID) (Harvard Apparatus), and the aorta was ligated. The trachea was cannulated with a 16G cannula (McMaster-Carr), and the right main bronchus was ligated. Subsequently, the right upper, middle, and lower lobes were tied off and removed. Decellularization was performed by sequentially perfusing the PA (constant pressure, 40 mm Hg) with heparinized (10 units/mL) phosphate-buffered saline (PBS, 10 min), 0.1% sodium dodecyl sulfate (SDS) in deionized water (2 h), deionized water (15 min) and 1% Triton X-100 in deionized water (10 min). The resulting scaffolds were washed with PBS supplemented with 1% antibiotics and antimycotics for 72 h to remove residual detergent and cellular debris. All reagents were sourced from Sigma-Aldrich. Scaffolds showing evidence of infection, vascular air trapping or vascular leakage were excluded from the study.

Incucyte proliferation assay

iECs were split and plated in 6-well plates in Vasculife culture media with final concentration of 20.000 cells/cm^2. After O/N culture, media were changed according to culture protocol and iECs were cultured in angiogenic medium (AM), modified stabilization medium (MSM) and Vasculife medium (Vasculife) as control, until the control group reached confluence. After O/N culture, Incucyte Live-Cell Analysis System acquired multiple images from each well for each condition to calculate the confluence at the starting point (T0). In addition, images were acquired every 6 h until the control group reached the 100% confluence.

Tube formation assay

The assay was performed according to the manufacturer's protocols of Corning Matrigel Matrix. Briefly, Matrigel thawed overnight at 4°C was mixed with VEGF (200 ng/mL) and 250 μL of matrix was added to each well of 24-well plates. After 1h of incubation at 37°C, iECs (10 × 10^5) were seeded onto the Matrigel. Tube formation was observed for 16 h in several culture media, i.e., Vasculife medium (Vasculife), AM, MSM or the iVEP two phase culture media protocol (11.5 h of AM + 4.5 h of MSM, 70% + 30% of the culture time, respectively). To mimic the two-phase culture media protocol, all groups were exposed to the same medium firstly for 11.5 h and subsequently for 4.5 h. Cells were rinsed every media change. Analyses were performed at the end of the follow-up, using an inverted phase-contrast microscope to investigate tube formation. ImageJ Angiogenesis software was used for the quantification of mesh size.

Dynamic insulin secretion test (IST) of ViβeS

To assess insulin secretion after *in vitro* culture of ViβeS, an insulin secretion test (IST) was performed on day 7 of culture. The dynamic IST was performed as previously described.[65] Briefly, Viβes were loaded in a perfusion chamber for suspension cells and connected to a high-capacity, automated perifusion system (BioRep Perifusion V2.0.0). The flow rate was set to 0.2 mL/min and the assay was performed at 37°C environment. ViβeS were initially perfused with a low glucose insulin-free perifusion buffer (0.5 mM glucose) for 20 min to allow β cells equilibration and removal of culture medium. Next, Viβes were stimulated with insulin-free perifusion buffer at 11 mM glucose for 20 min. Samples of the effluent were collected at baseline and every minute from minute 0 to +20 of stimulation. All samples were frozen at −20°C until assayed for insulin content (Mercodia Insulin ELISA Kit, 10-1113-10). The dynamic insulin release results were compared using the following parameters: insulin release as determined by the area under the curve (AUC, calculated by the linear trapezoid method expressed in fold change over the basal of the insulin release), AUC mean of the peak at interval 2–7 min.

In vitro seeding and culture of iVEPs

As previously described[23] decellularized left lung lobes were mounted in a custom-made bioreactor with PA cannula and PV cannula attached to individual perfusion circuits and the trachea cannula attached to a reservoir that was about 25 cm (20mmHg) above the level of the PA. The trachea was kept open to the inside of the bioreactor and closed to the reservoir through a three-way valve 5 cm above the level of PA. iVEPs were engineered following a two-phase seeding protocol: 1) For endothelial delivery through the PA and PV, 30x10^6 iEC were re-suspended in two separate seeding chambers (each with 15 x10^6 iECs) in 80 mL of AM and seeded simultaneously through the PA and PV under 30 mmHg gravity. The organ was cultured under static conditions for 2 h. Perfusion was initiated at 0.5 mL/min from both the PA and PV. For tracheal seeding, the PV cannula was released, the trachea opened to the reservoir and closed to the chamber on day 1 of culture. 2x10^6 SC-islets (Corresponding to 2000 AC of ViβeS) were re-suspended with 10x10^6 of iECs in 50 mL of AM and seeded from the tracheal reservoir, followed by 200 mL AM. Static culture for 2h completed airway seeding and before starting perfusion. To re-initiate perfusion, the trachea was opened to the chamber and flow was set to 1 mL/min from the PA. iVEPs were cultured for a total of 7 days with the initial 5 days in AM and subsequent 2 days in MSM at 37°C in 5% CO2. iVEPs were harvested for functional and histological assessment on day 7. For *in vivo* transplantation iVEPs were used at day 7.

In vitro FITC-Dextran assay

FITC-Dextran assay was performed on mature iVEPs. iVEPs were perfused at 1 mL/min with DPBS then at min 3 a 1 mL of solution of (5 mg/mL) FITC-Dextran at 1 mL/min was injected and iVEPs were further perfused with DPBS. Eluate was collected at different time points (from 1 to 15 min) and dextran concentration was quantified.

Fluorescence microangiography

Fluorescence microangiography was performed on matured iVEPs, which were submerged in PBS at 37°C. 5 mL of 1% low melting point agarose (Invitrogen) in PBS containing 1:10 diluted blue FluoSpheres (0.2 μm, 365/415 Invitrogen) manually injected into the PA (about 5 mL/min). PA perfusion pressure was below 20 mmHg (PressureMAT Single-Use Sensor). Immediately after microangiography, iVEPs were moved to ice, to allow the agarose to solidify.

Dynamic insulin secretion tests (IST) of iVEPs

We tested iVEPs after 7 days of culture. iVEPs were mounted on a custom-build *in vitro* perfusion device as follows: the iVEP was placed on a platform in a prone position with the PA cannula connected to a perfusion line, the PV cannula open to the level of the PA allowing collection of venous drainage, and with the trachea open 5 cm above the PA. Insulin secretion of iVEPs was measured using a modified IST protocol.[65] iVEPs were perfused with the previously described perifusion buffer at 0 mM glucose for 40 min to eliminate the insulin stored during the 7 days of culture, later at 0.5 mM glucose for 20 min to allow equilibration. Next, iVEPs were stimulated with 11 mM glucose for 20 min. Samples were collected from venous drainage at baseline and from minute 1 to 20 of stimulation. The IST was performed with 1 mL/min perfusion at 37°C and 5% CO2. All samples were frozen at −20°C until assayed for insulin content (Insulin ELISA Kit, code:10-1113-10, Mercodia). The dynamic insulin release results were compared using the following parameters: insulin release as determined by the area under the curve (AUC calculated by the linear trapezoid method expressed as fold change over the basal of insulin release), first insulin phase (mean of the peak value at interval 0/+6), and second insulin phase (mean of the peak value at interval +6/+9).

miR-375 analysis and quantification

We measured miR-375 release and quantified the β cell loss during the iVEP maturation. To rule out biases related to the miRNA contribution of iECs, miR-375 was also quantified in iVEPs seeded with iECs only. Briefly, supernatants were sampled from 100 mL of iVEPs culture media in DNA/RNA LoBind microcentrifuge tubes (Eppendorf, Hamburg, Germany), stored at −80°C and then extracted using either the NucleoSpin miRNA Plasma kit (Macherey-Nagel, Düren, Germany), or the Maxwell RSC miRNA Plasma and Serum Kit (Promega, Madison, USA) according to the manufacturer's instructions. 100 ACs of ViβeS and 100,000 iECs were pelleted and stored at −80°C, lysed in ML lysis buffer from the Nucleospin miRNA kit (Macherey-Nagel, Düren, Germany), used for the subsequent small + large RNAs extraction. Eluted RNA from cells was quantified using the Epoch Microplate Spectrophotometer (BioTek Instruments, Inc., Winooski, VT, USA). cDNA was obtained by reverse transcription of 5 μL or 10 ng of extracted RNA from supernatants or cells miRNA respectively, using the TaqMan MicroRNA Reverse Transcription kit (Applied Biosystems, Foster City, USA). A mix of diluted reverse-transcription primers, specific for human miR-375 (hsa-miR-375: assay ID 000564 Life Technologies, Carlsbad, USA) and miR-16 sequences (hsa-miR-16: assay ID 000391), was used as 5× reverse transcription primer, as indicated by the manufacturer's protocol. miR-375 and miR-16 (as quality control) were quantified by droplet digital PCR (ddPCR) using the QX100 ddPCR system (Bio-Rad, Hercules, USA) as already described.[66] The optimal amount of cDNA for each ddPCR was previously established and corresponded to 5 μL and 2 μL of cDNA from supernatants and to 0.5 ng and 1 ng of cDNA from cells for miR-375 and miR-16, respectively. The concentration of target miRNA copies in the supernatant was obtained by correcting for the starting volume and for the fraction of extracted RNA and cDNA used in each reaction. Target miRNA copies per cell were determined by correcting for the ng of RNA input, the total amount of extracted RNA and the number of cells in the original sample. Based on the estimated number of miR-375 copies per cell and the miR-375 copies measured in the iVEP supernatants at each time-point, we calculated the percentage of β cells lost during the iVEP maturation process.

Diabetes induction and metabolic monitoring

Diabetes was induced by alloxan (72 mg/kg i.v., Sigma-Aldrich) administrations in NSG mice 2 days before transplantations.[67–69] Animals with non-fasting glucose <450 mg/dL prior to transplantation were not considered diabetic and excluded from the study. Diabetes reversal was defined as 3 consecutive glycemia measurements ≤200 mg/dL and maintained until the end of follow-up. iVEP graft function was assessed daily through non-fasting blood glucose measurements using a portable glucometer (OneTouch Ultra, Bayer) after transplantation. Exogenous insulin therapy (LinBit pellet; LinShin) was administered subcutaneously peri-transplant to maintain an acceptable healthy status.[50] The day after transplantation a suboptimal quantity of 2 pellets were implanted in all diabetic recipients with a non-fasting glycemia >250 mg/dL. No pellets were implanted in animals with sustained function and non-fasting glycemia ≤250 mg/dL. One pellet was removed 10 days after transplantation and the second one 20 days after transplantation.

Device-less subcutaneous transplant site generation and ViβeS transplantation

NSG recipient diabetic mice were anesthetized with Avertin (tribromoethanol) (intraperitoneal injection at a dose 0.75 mg/g; Sigma). As described by Pepper,[58] 3 to 6 weeks before transplant, the device-less (DL) site was created by implanting a 2 cm segment of 5-French (Fr.) textured nylon radiopaque angiographic catheter (Cook Medical, Indiana, USA) subcutaneously into the lower left quadrant of 20–25 g female recipient NSG mice. At the time of transplantation, a small (4 mm) incision was made to gain access to the catheter. The tissue matrix surrounding the superior margin of the catheter was dissected to withdraw and remove the catheter. 2000 ViβeS containing $2x10^6$ SC-islets were aspirated into polyethylene (PE-50) tubing, using a micro-syringe and centrifuged into a pellet suitable for transplantation. ViβeS were carefully injected into the subcutaneous pouches using the micro syringe (Hamilton). The incision was closed with surgical silk suture (Ethicon, New Jersey, USA).

iVEPs implantations in diabetic recipient mice

Female NSG diabetic recipients were anesthetized (22–26 gr) with Avertin (tribromoethanol) (intraperitoneal injection at a dose 0.75 mg/g; Sigma). Prior to mice implantation, iVEPs were flushed with 150 mL ice-cold DMEM (GIBCO- 5.5 mM glucose) from the PA. Next, iVEPs were carefully dissected from the heart and trachea and divided with a sagittal incision into 2 segments. iVEPs segments were implanted in 2 separate subcutaneous pockets generated on the dorsal left and right area. The single pocket was specifically created by 210-mm lateral transverse incisions limiting a 2 cm tunneled area. Once iVEPs were placed in the dedicated space, the implant was ligated under the skin with 2 prolene sutures (Ethicon, New Jersey, USA) by sides and skin incision was closed with a surgical silk suture (Ethicon, New Jersey, USA).

Oral glucose tolerance test

An oral glucose tolerance test (OGTT) was performed on NSG transplanted with iVEPs and DL-ViβeS at 4 weeks after transplantation. 1 g/kg of glucose was administrated by oral gavage after 4-h fast. Blood glucose was determined at 0, 10, 20 30, 60, 90, and 120 min after glucose administration. The area under the curve (AUC) of glucose during OGTT was calculated using the trapezoidal method (baseline = 0 min).

iVEPs vessel density and dextran assay

iVEPs vascular density was quantified as previously reported.[22] Briefly, iVEPs segments were explanted 30 days after implantation were explanted and 32-bit color images were acquired. Explant samples presenting surgical damage were excluded from the analysis. The images were processed by the unbiased AngioTool software,[70] generating an analysis that includes segmentation, skeletonization and analysis of the vasculature. On iVEPs image, AngioTool 64 version 0.6a identifies vessel profiles according to the software's preset parameters. Identified vessels are demarcated with an outline on the image displayed. Once the outline overlay matches the vessels in the displayed image, the analysis can be carried out. On completion of the analysis, the resulting image shows an overlay, which indicates the area encompassing all vessels, a skeletal representation of the vascular network and the computed branching points inside this area. This image represents the explant area, the outline of the analysis, the vessels, and their branching point, is saved together with an Excel file containing the analysis parameters and the computed results (explant area, vessel area, percentage surface vessel density, total number of junctions, junction density, total vessel length, average vessel length). At the end of the follow up (13 weeks), heart beating NSG recipients were infused i.v with 200 μl of FITC-Dextran solution (20 mg/mL). 30 min post infusion iVEPs were harvested and samples were analyzed in immunofluorescence.

Flow cytometry

iECs/SC-islets were stained for 30 min at 4°C in a dark place with Live Dead Pacific Blue dye (Life Technologies) using 1 μL of dye every 1×10^6 cells resuspended in 1 mL of PBS. Live Dead dye is able to stain dead cells in order to select the population of living cells. Cells were stained for 20 min with primary antibodies in the dark at 4°C: anti-human CD31-APC-Cy7 (Biolegend), anti-human CD90 APC (R&D Systems), anti-human CD105-FITC (BD Biosciences), anti-human CD73-PE (BD Pharmingen), anti-human PDX1-Alexafluor488 (BD Pharmingen), anti-human NKX6.1-PE (BD Pharmingen), anti-human INSULIN-AlexaFluor647 (BD Pharmingen). Samples were fixed with 200μL cytofix/cytoperm buffer (ThermoFisher) for 20min. Before every step, samples were washed with FACS Buffer (PBS supplemented with 0.2% of BSA) and centrifugated at 1200 rpm for 8 min. Samples were acquired on a FACSCantoII instrument (BD Biosciences) or a Cytoflex S/LX. Calibration beads (Life Technologies) were used to calibrate and normalize acquisition settings in each experiment. Flow cytometry data were analyzed using FlowJo 10.6.2. Software.

Histology and immunostaining

All samples were fixed overnight with 4% paraformaldehyde in PBS (PFA) unless stated otherwise. For paraffin-embedded samples, 5 μm sections were used for histological analysis. For H&E staining, sections were deparaffinized, rehydrated, stained with hematoxylin QS (Vector Laboratories) and eosin Y (Fisher Scientific), and mounted with Permount (Fisher Scientific) after dehydration. For immunofluorescence staining, sections were deparaffinized, rehydrated, put through heat-induced antigen retrieval, permeabilized with 0.1% Triton X-100 in PBS, washed 3 times in DPBS blocked with 1% bovine serum albumin in PBS. Sections were incubated in primary antibodies overnight at 4°C. Primary antibodies included antibodies against human CD31 (1:50, DAKO, M082301), human CD144 (1:100, R&D systems AF938), human Von Willebrand Factor (1:200, DAKO A0082), human Chromogranin

A (1:200, ABCAM A15160 or 1:100 Invitrogen MA513096), human Insulin (ready-to-use, Agilent IR00261-2), and against mouse CD31 (1:100, Cell Signaling 77699S; 1:100 BD Pharmigen AB_393571). After overnight incubation, sections were washed 3 times with PBS and then incubated in Alexa Fluor 488, Alexa Fluor 547 or Alexa fluor 647-conjugated secondary antibodies (1:500; life technologies) for 40 min at room temperature, followed by 10 min staining with DAPI (1:500) and then 3 washes in PBS. Microangiography samples were fixed in PFA for 2 h, equilibrated in 30% sucrose in PBS overnight, and embedded in O.C.T. compound (Tissue-Tek). 50 μm cryo-sections were prepared for staining.

QUANTIFICATION AND STATISTICAL ANALYSIS

Values are summarized as mean ± SD (or SEM, where indicated). The Mann-Whitney U test was used to compare median values between 2 groups, while Welch t-test was performed to compare the AUC values of insulin release across different groups. Gain of normoglycemia was evaluated by Kaplan-Meier analysis, and differences between survival curves were estimated using the log rank test, while general linear model for repeated measures was used to estimate differences between groups for the *in vivo* follow-up. Statistically significant differences were defined as $p < 0.05$. Microsoft Excel 2011 (Microsoft Corporation, https://www.microsoft.com) and Graphpad Prism v10 (GraphPad Software, http://www.graphpad.com) and SPSS v20 (statistical package for Windows SPSS Inc., https://www.ibm.com/it-it/products/spss-statistics) were used for data management, statistical analysis and graph generation.